

**A MAJOR PROJECT REPORT ON  
NUMERICAL MODELLING ON SLOPE STABILITY  
SUBMITTED IN PARTIAL FULFILLMENT OF THE REQUIREMENTS  
FOR THE AWARD OF THE DEGREE OF  
MASTER OF TECHNOLOGY  
IN  
CIVIL ENGINEERING  
WITH SPECIALIZATION IN  
GEOTECHNICAL ENGINEERING  
BY  
MOHIT CHANDRA  
ROLL NO. 2K14/GTE/11  
UNDER THE SUPERVISION OF  
DR. RAJU SARKAR  
ASSISTANT PROFESSOR  
CIVIL ENGINEERING DEPARTMENT  
DELHI TECHNOLOGICAL UNIVERSITY**



**DEPARTMENT OF CIVIL ENGINEERING  
DELHI TECHNOLOGICAL UNIVERSITY**

**2016**



## **DELHI TECHNOLOGICAL UNIVERSITY**

### **CERTIFICATE**

This is to certify that project report entitled “NUMERICAL MODELLING ON SLOPE STABILITY” is a bonafide record of work carried out by Mohit Chandra (2K14/GTE/11) under my guidance and supervision, during the session 2016 in partial fulfilment of the requirement of degree of Master of Technology (Geotechnical Engineering) from Delhi Technological University, Delhi.

To the best of my knowledge, the matter embodied in the thesis has not been submitted to any other University/Institute for the award of any Degree or Diploma.

Dr. Raju Sarkar

Assistant Professor

Department of Civil Engineering

Delhi Technological University

Delhi-110042

2016



## DELHI TECHNOLOGICAL UNIVERSITY

### ACKNOWLEDGEMENT

I would like to express my deepest sense of gratitude and indebtedness to my guide and motivator **Dr Raju. Sarkar**, Assistant Professor, Civil Engineering Department, Delhi Technological University for his valuable guidance and support in all the phases from conceptualization to final completion of the project.

I wish to convey my sincere gratitude to Prof. Narendra Dev H.O.D. and all faculties of civil engineering department who have enlightened me during the project.

I am deeply thankful to my senior Ankur Mudgal who have helped me conducting the experiments.

I would always like to thank my parents for their encouragement and persistent support which has helped me to do better in all my endeavours.

Last but not the least; I would like to thank all the people directly and indirectly involved in successful completion of this project

MOHIT CHANDRA

ROLL. No 2K14/GTE/11

## CONTENTS

Table of contents.....	4
List of figures.....	7
List of tables.....	10
Abstract.....	11

## TABLE OF CONTENTS

CHAPTER 1 : INTRODUCTION .....	12
1.1 Introduction:.....	12
1.2 LEM (Limit equilibrium method).....	14
1.3 FEM (Finite element method).....	14
1.4 Numerical modelling: overview .....	15
1.5 Objective:-.....	15
CHAPTER 2: LITERATURE REVIEW .....	16
CHAPTER 3: NUMERICAL MODEL .....	20
3.1 Introduction.....	20
3.2 Actual model in laboratory .....	21
3.3 Geotextile used.....	23
CHAPTER 4: EXPERIMENTAL STUDIES .....	25
4.1 Scanning Electron Microscope (SEM) .....	25
4.2 Tensile test of geotextile .....	26

4.2.1 Grab tensile test (ASTM D4632).....	26
4.2.2 Wide width tensile test (ASTM D4595) .....	26
4.2.3 Tension creep test (ASTM D5262 AND D6992) .....	26
4.3 Specific gravity-.....	27
4.4 Sieve analysis.....	28
4.5 Standard Proctor test.....	29
4.6 Direct shear test.....	30
4.7 Triaxial test.....	32
CHAPTER 5: RESULT ANALYSIS .....	33
5.1 SEM .....	33
5.1.1 Geotextile A.....	33
5.1.2 Geotextile B .....	33
5.2 Tensile test of geotextile .....	34
5.2.1 Geotextile A.....	34
5.2.2 Geotextile B .....	35
5.3 Specific Gravity .....	37
5.4 Sieve analysis.....	37
5.5 Standard proctor test .....	38
5.6 Direct shear test.....	39
5.6.1 Direct shear test of soil .....	39
5.6.2 Direct shear test of soil sample with woven geotextile.....	39
5.6.3 Direct shear test of soil with Non woven geotextile.....	41

5.7 Triaxial test.....	43
5.7.1 UU of soil.....	43
5.7.2 UU of soil with woven geotextile.....	43
5.7.3 UU of soil with Non woven geotextile.....	44
5.8 Numerical simulation.....	44
5.8.1 Model at 45 <sup>0</sup> slope angle.....	44
5.7.2 Model with Geotextileat 45 <sup>0</sup> slope angle.....	48
5.9 Model aat 60 <sup>0</sup> .....	50
5.9.1 Model at 60 <sup>0</sup> slope angle.....	50
5.9.2 Model with Geotextileat 60 <sup>0</sup> slope angle.....	52
CHAPTER 6:RESULTS AND DISCUSSION.....	55
6.1 Test result for 45 <sup>0</sup> .....	55
6.2 Test result for 60 <sup>0</sup> .....	57
CHAPTER 7: CONCLUSION .....	60
REFERENCES .....	61

## LIST OF FIGURES

<b>FIG. NO</b>	<b>TITLE</b>	<b>PAGE NO.</b>
Fig.1	Concept model	20
Fig.2	Model in laboratory	21
Fig.3	Slope before failure	21
Fig.4	Model with gravity loading	22
Fig.5	Model with slope failure	22
Fig.6	Model with failure surface	23
Fig.7	Geotextile A	23
Fig.8	Geotextile B	24
Fig.9	SEM machine	25
Fig.10	Tensile test of geotextile	27
Fig.11	Standard proctor test	30
Fig.12	Direct shear testing machine	31
Fig.13	SEM of geotextile A at 1mm	33
Fig.14	SEM of geotextile B at 1mm	34
Fig.15	Grab tensile test	36
Fig.16	Particle size distribution of DTU soil	37
Fig.17	compaction curve of soil	38

Fig.18	Load-Displacement curve of soil	39
Fig.19	Shear stress-Normal stress curve of soil	40
Fig.20	Load-Displacement curve of soil with woven geotextile	40
Fig.21	Shear stress-Normal stress curve of soil woven geotextile	41
Fig.22	Load-Displacement curve of soil Non-woven geotextile	41
Fig.23	Shear stress-Normal stress curve of soil Non-woven geotextile	42
Fig.24	Stress-strain curve of DTU soil	43
Fig. 25	Stress-strain curve of DTU soil with woven geotextile	43
Fig.26	Stress-strain curve of DTU soil with Non-woven geotextile	44
Fig.27	Soil sample in Triaxial test	44
Fig.28	Schematic view of model with slope angle $45^0$	45
Fig.29	Deformed mesh of model with slope angle $45^0$	46
Fig.30	Total displacement of model with slope angle $45^0$	46
Fig.31	Total shear strain shading with scale with slope angle $45^0$	47
Fig.32	Factor of safety of model with slope angle $45^0$	47
Fig.33	Schematic view of model with geotextile with slope angle $45^0$	48
Fig.34	Deformed mesh of modelwith geotextile with slope angle $45^0$	48
Fig.35	Total displacement of model with geotextile with slope angle $45^0$	49
Fig.36	Total shear strain shading with geotextile with slope angle $45^0$	49



Fig.37	Factor of safety of model with geotextile with slope angle $45^0$	50
Fig.38	Deformed mesh of model with slope angle $60^0$	50
Fig.39	Total displacement of model with slope angle $60^0$	51
Fig.40	Total shear strain shading with scale with slope angle $60^0$	51
Fig.41	Factor of safety of model with slope angle $60^0$	52
Fig.42	Deformed mesh of model with geotextile slope angle $60^0$	52
Fig.43	Total displacement of model with geotextile slope angle $60^0$	53
Fig.44	Total shear strain shading with geotextile slope angle $60^0$	53
Fig.45	Factor of safety of model with geotextile with slope angle $60^0$	54
Fig.46	Load-settlement curve for $D/B=0$ with slope angle $45^0$	55
Fig.47	Load-settlement curve for $D/B=1$ with slope angle $45^0$	56
Fig.48	Load-settlement curve for $D/B=2$ with slope angle $45^0$	56
Fig.49	Load-settlement curve for $D/B=0$ with slope angle $60^0$	57
Fig.50	Load-settlement curve for $D/B=1$ with slope angle $60^0$	58
Fig.51	Load-settlement curve for $D/B=2$ with slope angle $60^0$	58
Fig.52	Maximum load capacity for different edge distance	59

## LIST OF TABLES

TABLE NO	TITLE	PAGE NO.
Table.1	Properties of geotextile	34
Table.2	Tensile test for Geotextile A	35
Table.3	Tensile test for Geotextile B	35
Table.4	Comparative properties of Geotextile	36
Table.5	Spesificgravity test results	37
Table.6	Sieve analysis of DTU soil	38
Table.7	variation of proctor compaction value	39
Table.8	Direct Shear test result	42
Table.9	Physical properties of soil	45

## LIST OF SYMBOLS

$C_c$  = coefficient of curvature

$C_u$  = coefficient of uniformity

$E$  = Efficiency factor

$S$  = shear strength

$\bar{\sigma}$  = normal stress on the plane of shearing

$C$  = Cohesion

$\Phi$  = interface friction angle

## **ABSTRACT**

In this study our aim is to carry out the analysis of slope stability of a man made slope by using PLAXIS software. The program provides a convenient graphical user interface that enables a quick generation of geometry model. The slope stability analysis consists determining the soil properties, the shape and the position of possible failure surface. The physical properties of soil used in model testing are evaluated from laboratory experiments and numerical simulation of physical model of slope. The study consists to determine the failure surfaces and corresponding factor of safety.

To determine FOS of a specified slope is highly dependent on the method of analysis used. As geotechnical engineer, it is a challenge to decide that which method can simulate better results. This thesis is limited to staged construction slope model and all the studied cases are taken from past researches that have been done all over the world.

## CHAPTER 1

### INTRODUCTION

#### 1.1 Introduction:

Slope stability is one of the major problem in geotechnical engineering. Slope instability is very common problem in natural soil slope, road and railway embankments, landfills, deep cuts etc. Normally, natural fill can be comprises of different soil layers like silts, sand, clay etc. Natural slope may lose their stability by sliding, road embankments may fail by detachment of soil particles and by losing their shear strength due to various environmental factor and different water conditions. Soil may undergo swelling and shrinkage due to climate variation results in settlement of soil and hence the settlement cause the failure of nearby infrastructure such as commercial and residential buildings. In road and railway embankments, failure occur in the form of cracking which causes the difficult driving conditions and also effects the rehabilitation cost throughout the country. So failure of slope is a major concern criteria to reduce the project cost and maintenance cost specially in road and railway projects, because finance is big problem in our country. These are some examples of slope failure which may cause loss of life.

Over the past decades, many research studies performed to provide various conventional methods to solve slope stability problems. In these methods main aim is to find factor of safety(FOS) to check liability of slope. Here FOS is defined as

$$FOS = \frac{\text{deriving shear stress}}{\text{resisting shear strength}}$$

There are three conditions-

- (i) FOS > 1 (resisting shear strength is greater than driving shear stress, slope is considered to be safe).
- (ii) FOS = 1 (resisting shear strength is nearly equal to driving shear stress, slope is liable to fail).
- (iii) FOS < 1 (slope is considered failed)

To analyse the slope, geotechnical engineer have to find the value of factor of safety for a particular problem. Analytically, the most common conventional method is limit equilibrium techniques. But now a days, commercial software like PLAXIS, GEOSLOPE etc. based on finite element method has made the powerful alternative for the assessment of such problems in geotechnical engineering field. Limit equilibrium method (LEM) and finite element method (FEM) are the two common techniques to handle such type of problems in geotechnical engineering field for designing and predicting mechanical behaviour of different slopes. The main advantages of finite element technique over convention limit equilibrium technique are that we can simulate complete interaction of structure foundation to the nearby soil and the failure plane, mode of failure can be predetermined.

In this report, a model of natural slope is prepared for the study. Staged construction of slope has been modelled and then loading conditions are applied. The parameters required for the modelling are used from various research papers. Soil used for the model preparation is locally available DTU soil.

PLAXIS software is based on finite element method and specially designed for the analysis of deformation and stability in geotechnical engineering projects. The simple graphical input

procedure enables a quick generation of complex finite element models and the enhance output facility provides a detailed presentation of computation results. The calculations are fully automated and based on robust numerical procedure. This concept make easier to work with the software just after a few hour training.

The model can be either plain strain or axisymmetric. It has a advantage to choose different type of soil model and can generate standard boundary condition automatically. For the calculation part, program offers three type of calculation for the user in each construction phase:- plastic, consolidation & safety. Results can be shown by load-displacement curves, stress path and stress-strain curves.

### **1.2 LEM (Limit equilibrium method)**

Basically LEM is a fairly efficient method in slope stability analysis and is being still used. The basic concept of the method is to divide whole soil mass into slices and calculate shear and normal forces for each slice by satisfying all the static equilibrium condition. Advantages of the method are – (1) it can provide FOS without any knowledge of initial condition. (2) There is no restriction on the slope of slip surface. Disadvantage of this method is that it does not consider stress-strain behaviour of soil for calculation.

### **1.3 FEM (Finite element method)**

There is no pre assumption about failure surface and failure planes. Complex and advance soil properties can be easily implemented. There is no assumption about slice forces (Griffiths and Lane 1999). It uses strength reduction method in which the reduction of shear parameter  $c-\phi$  progressed until the failure occurs.

The factor, total multiplier ( $\Sigma$ MSF) represents soil strength parameter in each phase of construction.

$$\Sigma\text{MSF} = \frac{C(\text{input})}{C(\text{reduced})}$$

MSF is set to 1 at the start of calculation afterward safety analysis starts through step procedure. The incremental multiplier with default no of 0.1 at the beginning is applied in order to determine amount of strength reduction and process is continues until all the additional steps are analysed. At final stage, the FOS is given by

$$FOS = \frac{\text{Available strength}}{\text{Strength at failure}} = \text{value of } \Sigma MSF \text{ failure}$$

#### **1.4 Numerical modelling: overview**

Numerical models are used to study changing behaviour of a particular model over time. These computer programmes represents the response of initial condition such as in situ stresses, water levels, boundary condition etc. Numerical model divides the whole soil mass into small zones. The results of numerical model can be easily compare with the empirical results. The method is mainly used to solve complex problems with complex condition which cannot be solve by using conventional methods.

#### **1.5 Objective**

- (1) To apply PLAXIS software to calculate FOS for unreinforced and reinforced slope.
- (2) To analyse the stability of unreinforced and reinforced slope on the basis of D/B ratios as 0, 1, 2.
- (3) To analyse the stability of unreinforced and reinforced slope on the basis of different slope angles.
- (4) Settlement analysis of reinforced and unreinforced soil slope in laboratory.
- (5) To simulate laboratory experimental results with PLAXIS software.

## CHAPTER 2

### LITERATURE REVIEW

**Chaulya and Singh (1998)** studied biological stabilisation of the dump slopes. They used Bamboo and Kashi two types of grass for biological stabilisation of the dump slopes. By numerical modelling it has been analysed that use of these grass in stabilisation significantly increase factor of safety of slope and have perform good role in maintaining long term stability.

**Crosta, Imposimato&Roddeman (2002)** studied floe like models used to simulate land slide instability and flow development. Their ideas was to implement elasto-plasticity with a linear elastic part and different applicable yield surface. They conclude that deposits comprises massive blocks and fine particles both. Deformation mechanism of such large scale flows are difficult to simulate on small scale testing. Numerical modelling can partially overcome these problems and can also predict landslide run out. The modelling is heavily depends on different factors like type of approach, physical model parameters, assumption and limitation of procedures and boundary condition.

**Change et al (2006)** said LEM has been used for single problems and its application to complex problem is limited. On the other hand FEM 2D analysis has alternative properties to solve complex problem. FEM analysis uses stress-strain behaviour of soil which was a problem in LEM. FEM changes problem from static indeterminate to statically determinate.

**Gorog and Torok (2007)** studied clayey slope by dividing it into two geotechnical units (impermeable and permeable). PLAXIS is used to simulate the slope and find circular and polygon slip surfaces.



**Khabbaz, Fatahi, and Nucifora (2007)** studied properties of heterogeneous slope, embankment slope over soft soil and slightly over consolidated clay. The results for respective parameters were studied and compared. They considered the effect of young's modulus of soil on safety factor. Their findings indicated that when simple homogenous slope is considered , the difference of safety factor is minimum. The comparative study of undrained and drained slope stability analysis , the FOS is lower for undrained condition. Elastic modulus (E) effects FOS results and deformation before failure.

**Heibum et al (2009)** studied that material behaviour of ground, water condition & soil structure interaction can be predicted better by FEM.

**Naeni, Rabe and Mahmoodi (2012)** studied the effect of geosynthetic reinforcing on clayey slopes. They did numerical study using finite element analysis on strip footing upon both unreinforced and reinforced clayey slopes. Their results shows variation of edge distances form slope , effect of different number of geosynthetic layer to obtain maximum bearing capacity and minimum settlement. It is also concluded that for both unreinforced and reinforced slopes, bearing capacity increases with increase in edge distance and as the soil friction angle increased, the efficiency of reinforcing reduced.

**Rouaiguia and Dahim (2013)** determined FOS based on limit equilibrium method (Morgenstern-Price method and Mohr-Columb method). Study considered the influence of internal angle of friction, cohesion, unit weight of soil. Investigation was done through a series of examples and results shows that FOS increases with increase in cohesion and internal angle of friction. But more water pressure and increase in unit weight of soil layer significantly reduces factor of safety.

**Sandok, Fouad and NaimaBenmebarek(2013)** studied a case study over the effect of geosynthetics over Sabkha soil in Algeria. Based on the in situ observations and the geotechnical investigation, numerical simulation were performed using software PLAXIS.

**Kainthola and Verma (2013)** did analysis of road cut highway slopes. Uncertainty is a major factor in designing the slope as an increase in one degree of slope might make the unstable and vice-versa. Conventional practices can not explicitly address the uncertainty condition. So this led to use advance methods of analysis as finite element method.

**Fawaz, Farah and Hagechade (2014)** analyse the slope stability based on numerical simulation by using PLAXIS software. The properties of soil used for study were found by laboratory experiments. Their aim was mainly to found failure surfaces and factor of safety for a particular slope. All the calculation was done by considering the factors effecting slope instability and propose some methods to strengthen the slope for better results.

**Khan and Abbas (2014)** carried out slope stability analysis of road embankment by finite element method software (PLAXIS). The model was prepared by using flyash as fill material and geogrids were installed under static condition. After numeric simulation of model, they recommend the use of these materials for future design of embankment under light weight. The calculation included safety factor against the slope of different embankment material. Their conclusion was that under static condition, normal slope reinforced with geogrids has better safety factor up to maximum extent as compared to other embankment material.

**Khanmohammadi and Hosseinitoudeshki (2014)** investigate the effect of water on slope stability. They consider plain strain condition of numerical modelling. Their result shows that water level does not affect the FOS of slope until it rises to the rupture surface of slope. Water level has no effect on shape and depth of sliding surface. After penetration of water, there is a sharp decline in FOS of slope.

**Eftekhari, Taromi and Saidi (2014)** studied a tunnel slope and analyse the effect of uncertainty on stability. Here uncertain condition include geotechnical missed details of exploration program, error in estimation of soil properties etc. they shows the importance of

precise and predetermined schedule for selecting site location, monitoring, complexities of geometrical model, uncertainty and its effect on stability of trench and the necessity of comprehensive slope management.

**Soren, Budi and Sen(2014)** analysed open pit slope and state stresses at critically instable failure zone, different failure mode and safe & functional design of excavated slope using numerical modelling technique. The purpose of analyses was to enhance our understanding of instable zones, investigation of potential failure mechanism, optimal slope design, reliability, economics and designing possible remedial measures. They conclude that finite element method is suitable for indication of stress-strain distribution in critically instable zone, displacement and plastic state of slope.

**Azzam and Elwakilb (2016)** studied the results of experiment and numerical modelling on the influence of soil confinement on the footing adjacent to slope. They perform tests with different model height, crest width, edge distance and found the ultimate bearing capacity of a circular footing rest on sandy slope. The studied parameters were slope angle and sub grade soil density. They uses cell-footing system to neglect the slope effect on the ultimate bearing capacity of footing and then numerical modelling analysis help to predict most probable failure mechanism.

## CHAPTER 3

### NUMERICALMODEL

#### 3.1 Introduction

A series of laboratory model test were conducted in a box with the dimension 1m x 0.5m in plan and 0.5m depth. The wall of box is made up of thick transparent fibre sheet and to ensure the rigidity the box is braced with steel strips along its edges on the outer surface. The transparent box is used so that we can clearly see the failure plain of slope model. The box was built sufficiently rigid so that it can maintain plain-strain condition and minimize the out of plain displacements. The inside wall of box is well polished to reduce the friction.

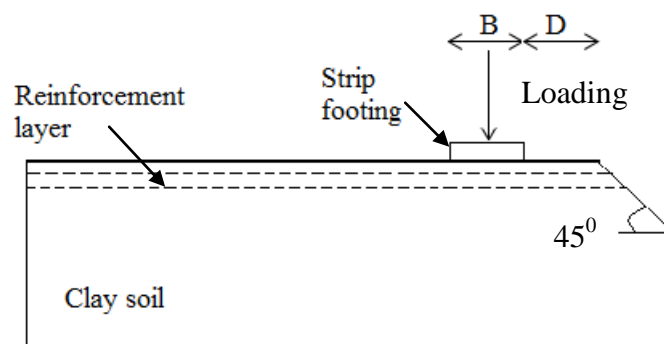


**Fig.1** Concept model

The model is prepared by staged construction technique. The load is applied by gravity loading using concrete cubes and beams. Soil used in model is compacted at its maximum dry density. The total soil used is around 350kg. Soil is collected from DTU campus.

Various analysis curves are obtained from laboratory testing. The load transfer mechanism can be shown by results of finite element analysis. Different plastic points are obtained by the method. The plastic failure zones of clayey slope are intercepted by reinforcing layer and stress distribution is extended much below it. This results in spreading the load into a wider area beneath the reinforcing zone, which is formed by a rigid region of soil and reinforcement is directly underneath the loaded area.

### 3.2 Actual model in laboratory



**Fig.2** Model in laboratory



**Fig.3** Slope before failure



**Fig.4** Model with gravity loading(Max. 1400 Kg)



**Fig.5** Model with slope failure



**Fig.6** Model with failure surface

### 3.3 Geotextile used

(A) This is a woven type of geotextile and is made up of polyester using weaving technique and have multifilament yarn filaments. During the process of weaving two parallel threads are interlaced at right angle.



**Fig.7** Geotextile A

(B) This is non-woven geotextile and is made up of polypropylene fibre. These are manufactures by randomly arranged fibre and bonded together in to a planer structure. The fibres are arranged into loose web and bonded together.

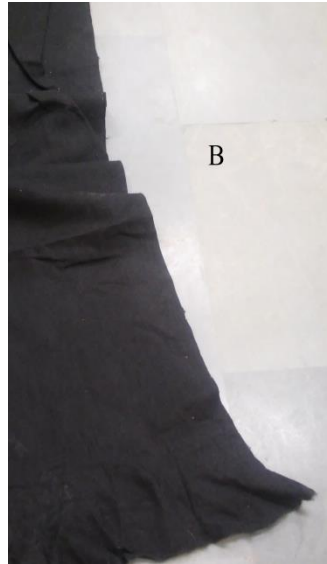


**Fig.8 Geotextile B**



## CHAPTER 4

### EXPERIMENTAL STUDIES

#### 4.1 Scanning Electron Microscope (SEM)

In this technique images are taken at microscopic level. A high energy beam of electron interacts with sample atom which produces signalling rays containing information about surface composition topography and electrical conductivity etc. In the standard detection mode (most commonly used mode), secondary electron imaging can produce very high resolution images of surface revealing information less than 1nm.

In SEM a wide range of magnification is possible about 10 times (equivalent to that of powerful hand lens) to 500,000 times. Back scattering electrons (BSE) are beam electron that are reflected from the sample. These are often used in SEM along with the spectra made from characteristic X-rays. The intensity of BSE is strongly related to the atomic number of specimen. These images can provide the information about distribution of different element in sample. X-rays are emitted when electron beam removed an inner shell electron from the sample, causing a higher energy electron to fill the shell. These X-rays are used to identify the composition of element in the sample.



**Fig.9** SEM Machine

## **4.2 Tensile test of geotextile**

### **4.2.1 Grab tensile test (ASTM D4632)**

It provides ultimate strength at failure. Non-woven geotextiles exhibit more strength when confined in end use application. In the test, each specimen is clamped by one inch jaw in the centre of width and pulled quickly. The test is easy, cheap and can be performed quickly. It gives the strength which verifies the quality and consistency of product during construction quality control.

### **4.2.2 Wide width tensile test (ASTM D4595)**

It takes longer to complete and is much more expensive than the grab test. In this test, the specimen is gripped along its full width and pulled slowly. The results are expressed as load per unit width. The test is more suitable for woven geotextiles. Here test data can be expressed in stress-strain curve, from which modulus values can be calculated. Stress-strain values and modulus values can be used to design woven geotextiles. This test does not result in a true design value for non-woven geotextile.

### **4.2.3 Tension creep test (ASTM D5262 AND D6992)**

It is a time-consuming test, in which a sustained load is applied on the specimen for up to 10000 hours (417 days). The creep deformation strain of the sample is monitored over the test period. From monitoring, we can determine the load level that will cause the rupture.

Considering all the factors, we have performed the Grab Tensile test to determine the properties of geotextile as modulus, stresses at yield point and break point for both woven and non-woven type geotextile.



**Fig.10** Tensile test of geotextile

### 4.3 Specific gravity

To determine the specific gravity of DTU soil .

Pycnometer was used.

If the volume taken of sample & that of reference substance is same, it is called as apparent specific gravity.

$$\text{Sp. Gr. (G)} = \frac{\text{Density of soil}}{\text{Density of water}} = \frac{M_2 - M_1}{(M_2 - M_1) - (M_3 - M_4)}$$

Where,  $M_1$  = mass of empty jar

$M_2$  = mass of jar containing dry sample

$M_3$  = mass of jar containing soil sample in water

$M_4$  = mass of jar with water only

#### 4.4 Sieve analysis

To determine the particle size distribution of DTU soil.

IS sieves of various sizes 4.75mm, 2.36mm, 1.18mm, 600 $\mu$ , 300 $\mu$ , 150  $\mu$ , 75 $\mu$ , pan and mechanical shaker were used to conduct the experiment.

The grain size analysis is an attempt to measure the different relative proportion of different grain sizes which make the whole soil mass.

In sieve analysis, sieves of opening of particular size are set over one another in decreasing order with sieve of largest opening at top and pan at bottom.

For determine the particle size distribution we are calculating the two coefficients-

(a) Coefficient of uniformity ( $C_u$ ) =  $\frac{D_{60}}{D_{10}}$

(b) Coefficient of curvature ( $C_c$ ) =  $\frac{D_{30}^2}{D_{60} \times D_{10}}$

Where  $D_{60}$  is grain size which passes 60% soil mass through,  $D_{30}$  is particle size such that 30% of soil mass is finer than it,  $D_{10}$  is the grain size which passes 10% soil mass through

To classify the soil according to their particle size distribution. It affects the permeability of soil mass and hence water condition in our model.

According to Indian standard condition for well gradation

$$1 < C_c < 3 \quad \text{for soil}$$

$$C_u > 6 \quad \text{for sand}$$

$$C_u > 4 \quad \text{for gravel}$$

#### **4.5 Standard Proctor test**

To determine optimum moisture content and maximum dry density of DTU soil.

Following apparatus were used.

- (1) Cylindrical mould having capacity 1000cc, internal dia. 100mm, height 127.3mm
- (2) Rammer having mass 2.6kg and drop height 310mm
- (3) Detachable base plate and collar
- (4) Balance with capacity up to 10kg
- (5) Drying oven and desiccators
- (6) Graduated jars, straight edge, spatula

Basically compaction is the process of densification of soil mass by reducing air voids. Sometime the process is confused with consolidation which is also a process of densification of soil mass but the difference is here, the expulsion of water takes place under continuous action of static load over long period.

The test is use to calculate the dry density in order to check the degree of compaction of soil mass. The degree of compaction is mainly depends on moisture content, compaction energy and type of soil. Every soil attains maximum dry density (MDD) at a particular compaction energy at particular moisture content known as optimum moisture content (OMC). In dry side, water act as a lubricant and helps in closer packing of soil grains and in wet side water starts to occupy the space of soil grains and restrict the closer packing of soil grains.

Soil density, shear strength and its bearing capacity is affected by degree of compaction. Compaction reduces voids, permeability, porosity and settlement. Results of the test are practically useful in problems like earthen dam, road embankments and airfields etc. In such construction degree of compaction is one the most important parameter. Moisture content in

the field for the particular soil is controlled by its optimum moisture content (OMC). Laboratory compaction test is useful to check the compaction specification in the field.

Precaution-

- (1) Water should be mix thoroughly with the soil.
- (2) Number of blows given to each layer should be uniformly distributed.
- (3) Each compacted soil layer should be scratched by spatula before placing next layer.
- (4) After the compaction of last layer soil should be 5mm above from the top of mould rim.
- (5) Compaction mould should be placed on solid foundation.



**Fig.11** standard proctor apparatus

#### **4.6 Direct shear test**

To determine  $c-\phi$  of DTU soil.

Direct shear test gives the value of internal friction of soil with or without geotextile. The geotextile specimens are cut using sharp cutting edge. A steel box divided into two parts

upper and lower. Testing specimens are placed into this box. Sandpaper is used at the base to prevent the stretching of geotextile. After clamping the lower box, the upper half must be clamping properly using pins. A known weight of soil sample then placed into upper half of shear box and compacted to a specified height by tamping to achieve the desired density. With the grid plate and top platen the shear box is placed into the loading frame carefully. After applying the testing loading, the specimen is sheared at a displacement rate of 0.125mm/min. In the assembly, lower box is covered entirely with geotextile hence no area correction is required. The test is performed for both soil with or without geotextile.

To determine internal friction angle of soil with or without geotextile and find the efficiency and interlocking of soil with geotextile. The internal friction angle is one of the major parameter concerning with slope instability.



**Fig.12** Direct shear testing machine

#### **4.7 Triaxial test**

To determine the effect of geotextile reinforcement on DTU soil.

Unconfined Undrained Triaxial test has been performed on DTU soil without reinforcement and with reinforcement. All test specimens were tested at cell pressure of 100 kN/m<sup>2</sup>, 200kN/m<sup>2</sup>, 250kN/m<sup>2</sup>. Woven and Non-woven reinforcement provided in two layers and placed horizontally in tested sample.



## CHAPTER 5

### RESULT ANALYSIS

#### 5.1 SEM

##### 5.1.1 Geotextile A

SEM of woven geotextile shows that both the layers are interlocked with each other. Fibre openings are at right angle to each other and regular. The aperture size is 0.2mm.

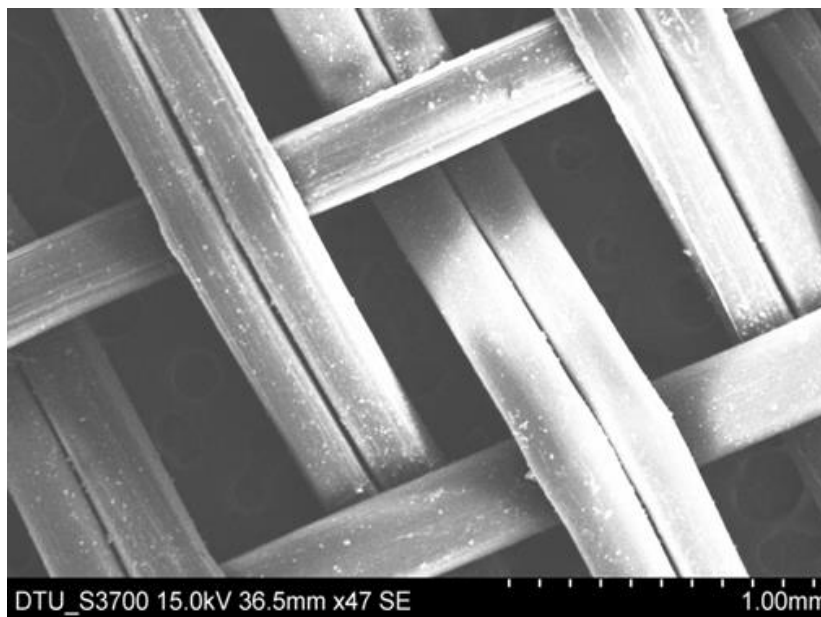


Fig.13 SEM of Geotextile A at 1mm

##### 5.1.2 Geotextile B

Non-woven geotextile fibres are arranged in random manner and interlocked to each other. The aperture size is 0.1mm.

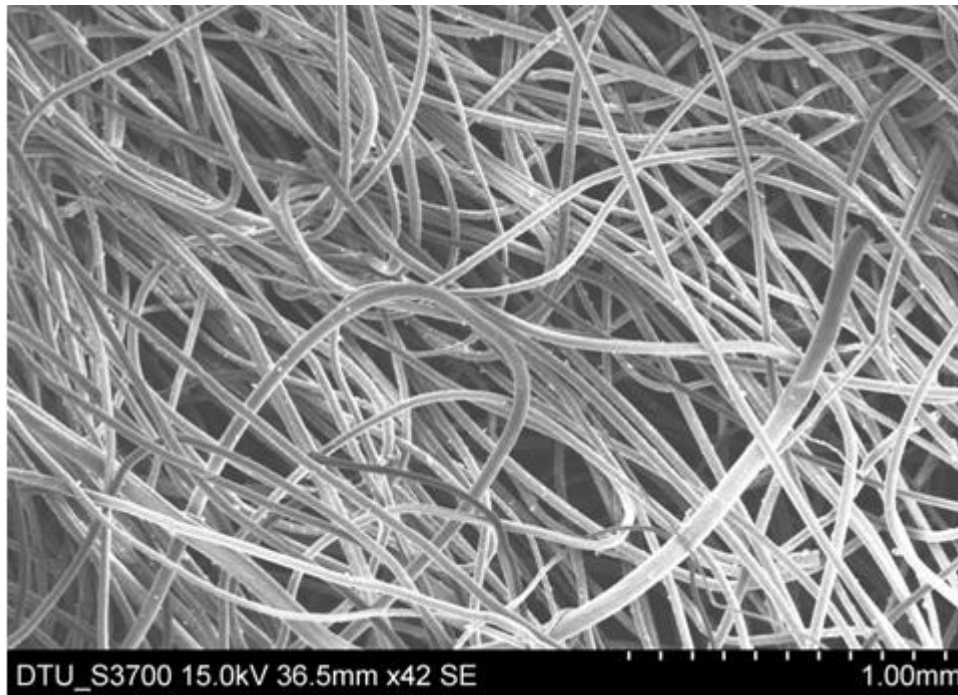


Fig.14 SEM of Geotextile B at 2mm

## 5.2 Tensile test of geotextile

**5.2.1 Geotextile A** :sample dimension length=200mm, width=100mm, thickness=0.93mm, modulus=33.24Mpa. stresses are calculated by-

$$\text{Stress at yield point} = \frac{\text{Maximum extension}}{\text{Original area}}$$

$$\text{Stress at break point} = \frac{\text{Maximum extension}}{\text{Final area}}$$

$$\% \text{ elongation} = \frac{\text{Maximum extension}}{\text{Original length}}$$

**Table.1** Properties of geotextile used.

PROPERTIES	WOVEN	NON-WOVEN
Specific Gravity	0.89	1.05
Thickness	0.3	0.45
Mass per unit area	140	450
Apert	0.7	0.04

**Table.2** Tensile test of Geotextile A

Maximum extension(mm)	105.2
Load at maximum extension (KN)	0.520
Original area (mm <sup>2</sup> )	92
Final area (mm <sup>2</sup> )	13.80
Modulus (Mpa)	33.24
Stress at yield point (Mpa)	5.58
Stress at break point (Mpa)	37.5
% elongation	0.30

**5.2.2 Geotextile B:** sample dimension length=200mm, width=100mm,thickness=0.74mm, modulus=14.11 Mpa.

**Table.3** Tensile test for Geotextile B

Maximum extension(mm)	170.48
Load at maximum extension (KN)	0.120
Original area (mm <sup>2</sup> )	74
Final area (mm <sup>2</sup> )	21.17
Modulus (Mpa)	4.11
Stress at yield point (Mpa)	1.62
Stress at break point (Mpa)	5.69
% elongation	0.85

**Table.4** Comparative properties of Woven and Non-Woven Geotextile

PROPERTY	WOVEN	NON-WOVEN
Breaking elongation	low	high
Breaking strength	high	low
Initial modulus	high	low



**Fig.15** Grab tensile test

### 5.3 Specific Gravity

The Specific Gravity of soil was found 2.60 by density bottle method.

**Table.5** Sp. Gravity results

Empty weight	M <sub>1</sub> (gm)	695.2	695.2	695.2
Empty weight+dry soil	M <sub>2</sub> (gm)	1201.1	1260.2	1210.4
Empty weight + dry soil + Water	M <sub>3</sub> (gm)	1878.5	1904.2	1880.5
Empty weight + water	M <sub>4</sub> (gm)	1566	1566	1566
Sp. Gravity	S.G.	2.61	2.59	2.58

### 5.4 Sieve analysis

Sieve analysis is done to determine particle size distribution of DTU soil and classify it on the basis Indian standard codes. The value of coefficient of uniformity( $C_u$ ) is 5.1 and coefficient of curvature( $C_c$ ) is 1.78. Where  $D_{10}=0.09$ ,  $D_{30}=0.24$ ,  $D_{60}=0.46$ . The soil is poorly graded.

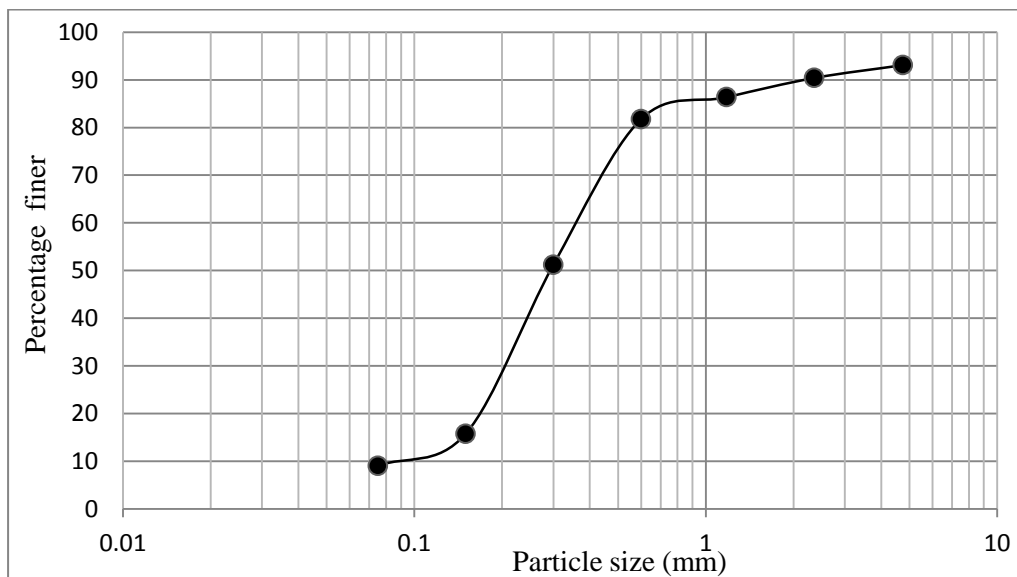


**Fig.16** Particle size distribution of DTU soil

**Table.6** sieve analysis of soil

Sieve sizes (mm)	Mass of Soil Retained	Percent Retained (%)	Cumulative Percent Retained	Cumulative Percent Finer (%)
4.75	69.1	6.91	6.91	93.09
2.36	26.9	2.69	9.6	90.4
1.18	61.5	6.15	15.75	86.35
0.6	25	2.5	18.25	81.75
0.3	305.5	30.55	48.8	51.2
0.15	354.5	35.45	84.25	15.75
0.075	67.1	6.71	90.96	9.04
pan	90.4	9.04	100	0

As per classification of Indian Standard code soil is classify as Silty sand(SM).

### 5.5 Standard Proctor test

Figure shows the relation between maximum dry density (MDD)and optimum moisture content (OMC).

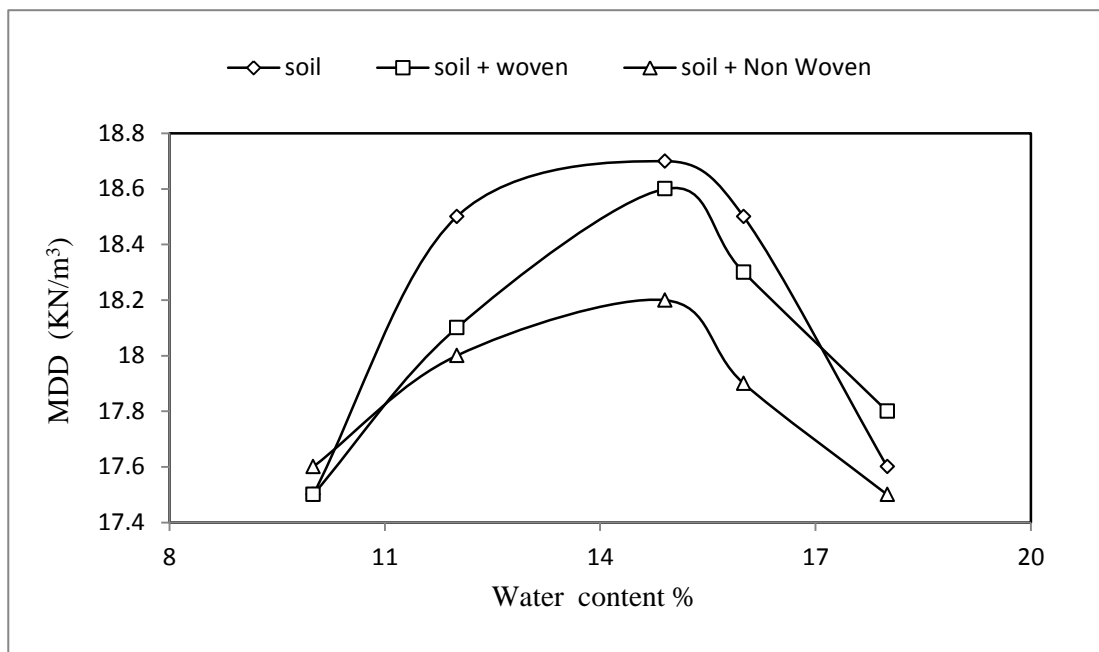


**Fig.17** Compaction curve of soil

**Table.7** variation of proctor compaction test with woven and Non-woven geotextile

PARAMETER	MDD (KN/m <sup>3</sup> )	OMC (%)
DTU soil	18.2	14
Soil + Woven geotextile	18.6	14.7
Soil + Non-woven geotextile	18.7	14.9

## 5.6 Direct shear test

### 5.6.1 Direct shear test of soil

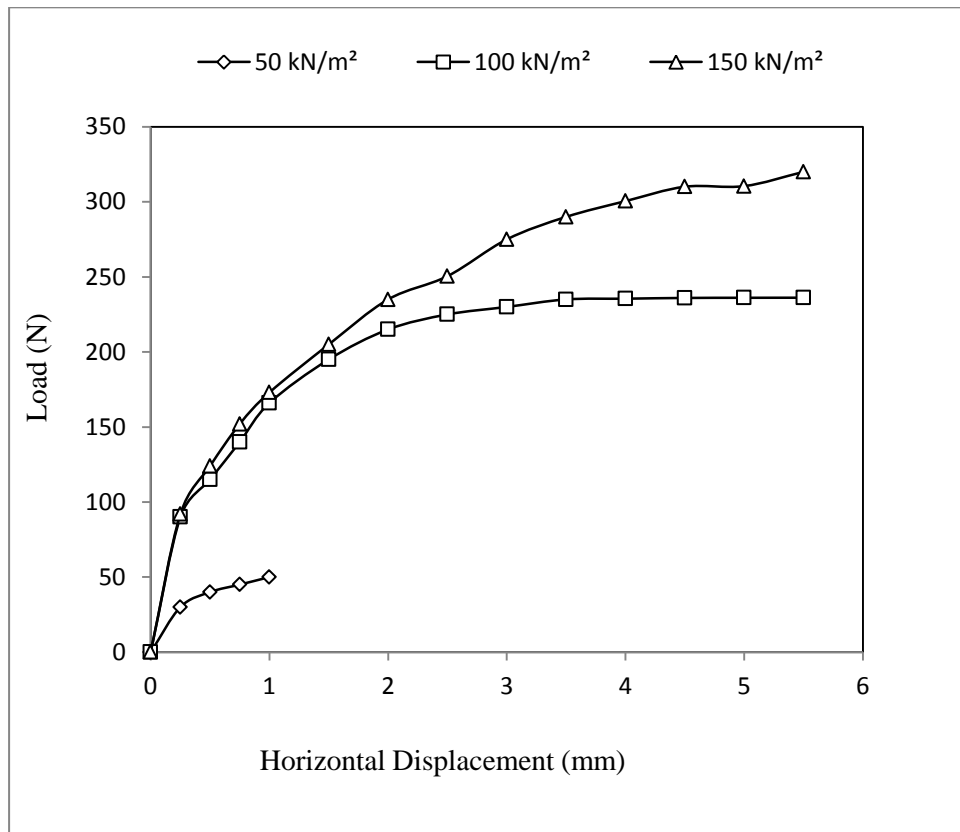


**Fig.18** Load displacement curve of soil sample

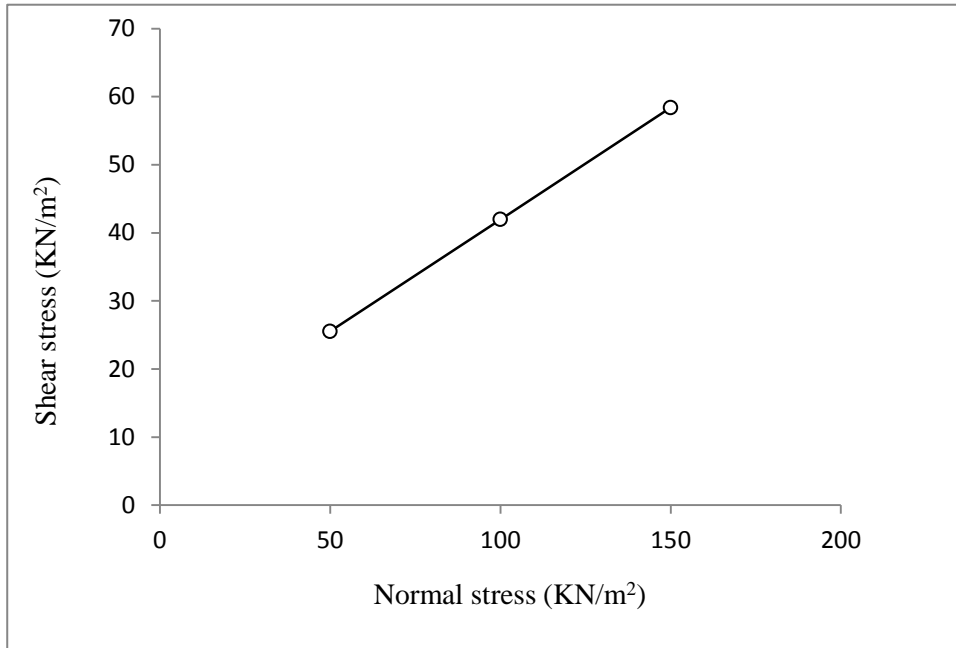


**Fig.19** Shear stress- Normal stress curve of soil sample

**5.6.2** Direct shear test of soil sample with woven geotextile placed at top and bottom.

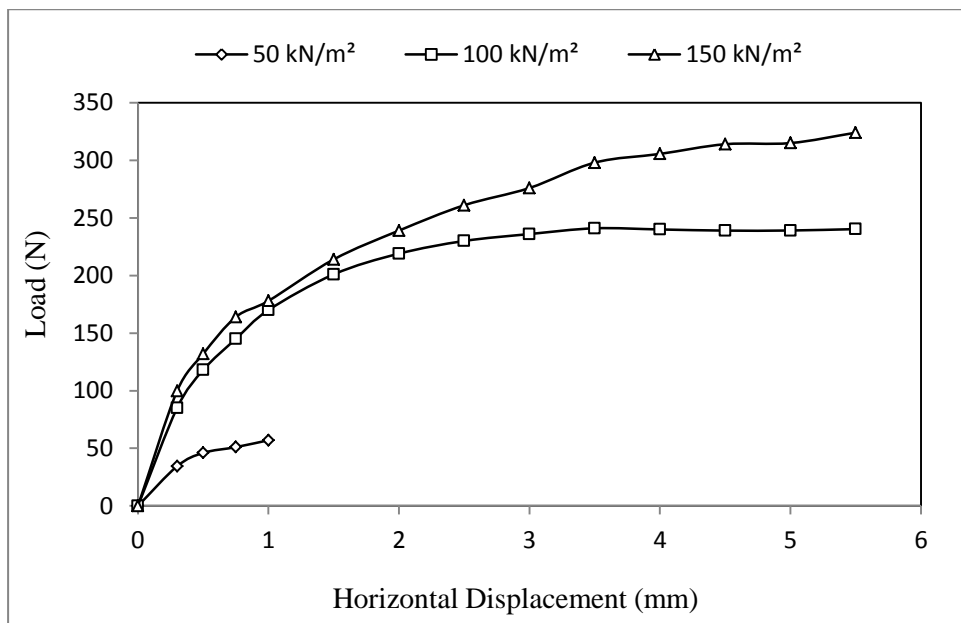


**Fig.20** load displacement curve of soil with woven geotextile



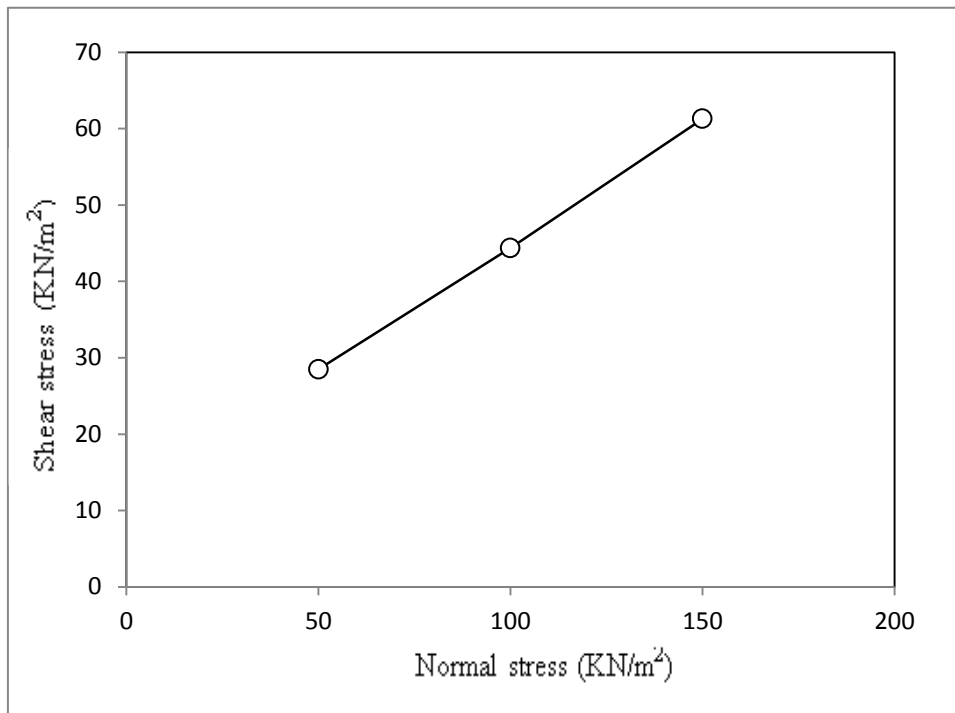


**Fig.21** Shear stress- Normal stress of soil with woven geotextile

**5.6.3** Direct shear test of soil with Non-woven geotextile placed at top and bottom

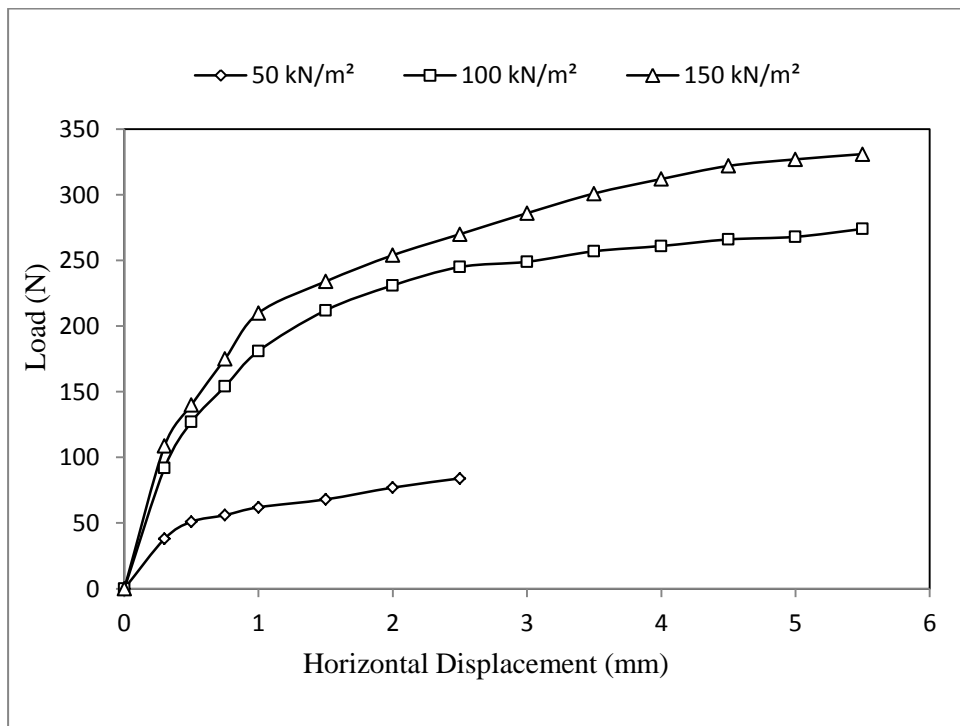


**Fig.22** Load displacement curve of soil with Non- woven geotextile

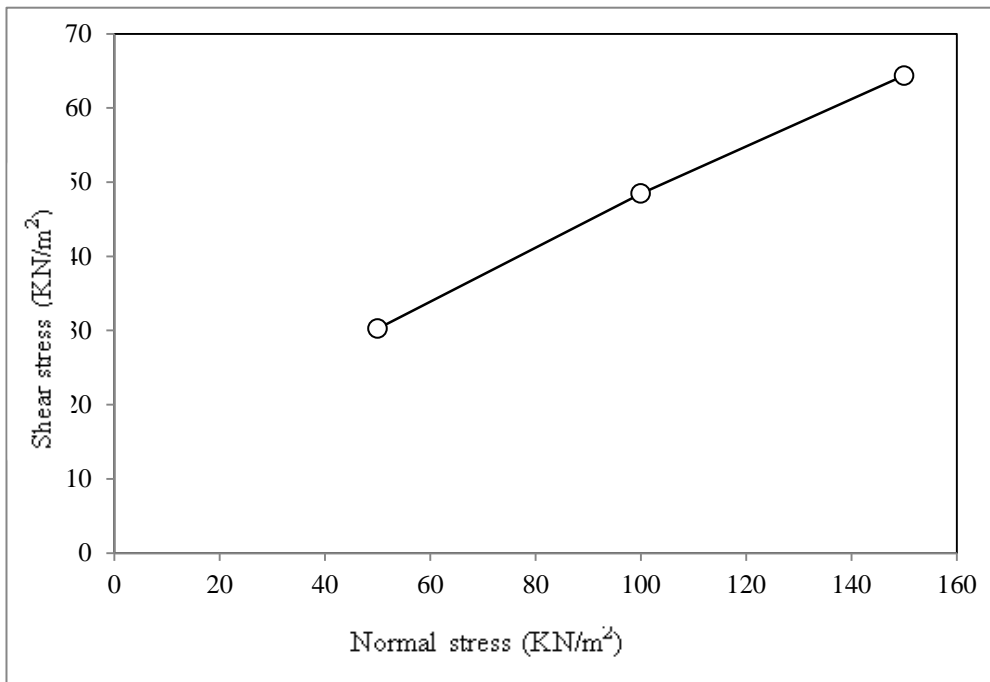


**Fig.23** Shear stress- Normal stress of soil with Non-woven geotextile

**Tble.8** Direct shear test results

<b>SAMPLE</b>	<b>C (kN/m<sup>2</sup>)</b>	<b>Φ (Degree)</b>
DTU soil	10.1	22.4 <sup>0</sup>
Soil + woven geotextile	11.2	19.9 <sup>0</sup>
Soil + Non-woven geotextile	12.6	19.4 <sup>0</sup>

## 5.7 Triaxial test results

5.7.1 UU test has been performed on soil sample for different confining pressures. It gives

$C=11.3\text{kN/m}^2$  and  $\Phi=18.5^\circ$ .

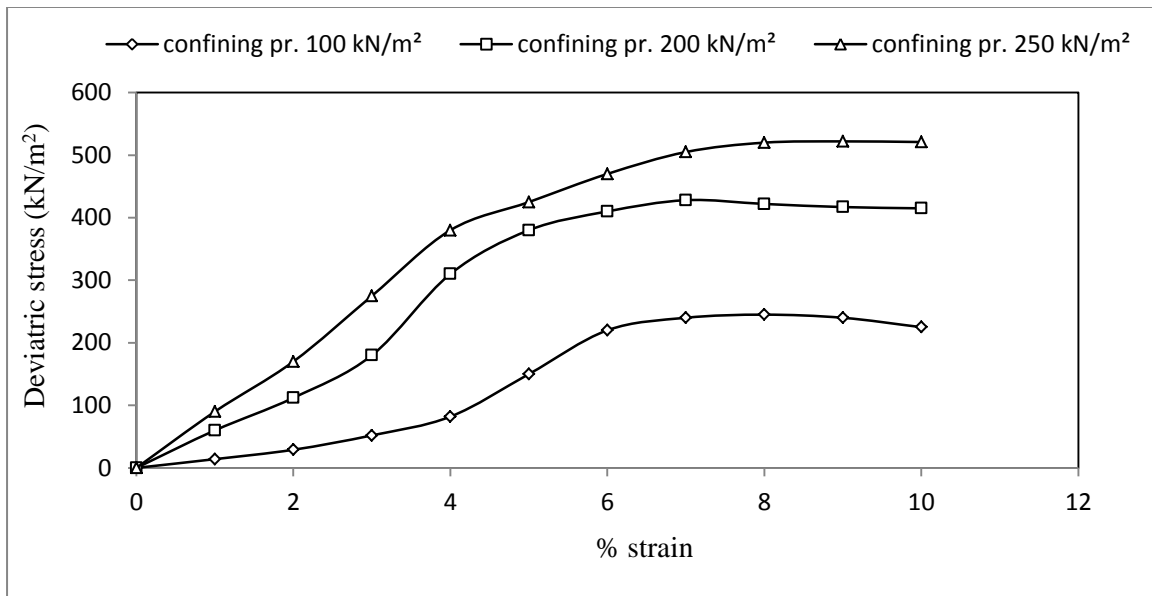


Fig.24 Stress-strain curve of DTU soil

5.7.2 UU test has been performed for soil with woven geotextile. It gives  $C= 15.8\text{kN/m}^2$  and

$\Phi= 19.4^\circ$ .

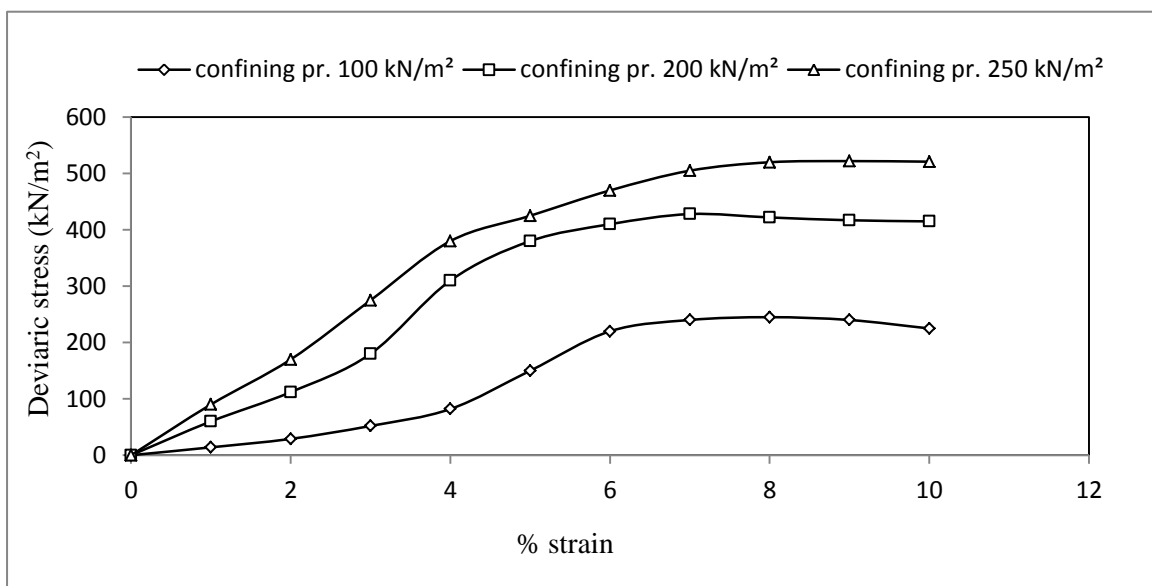
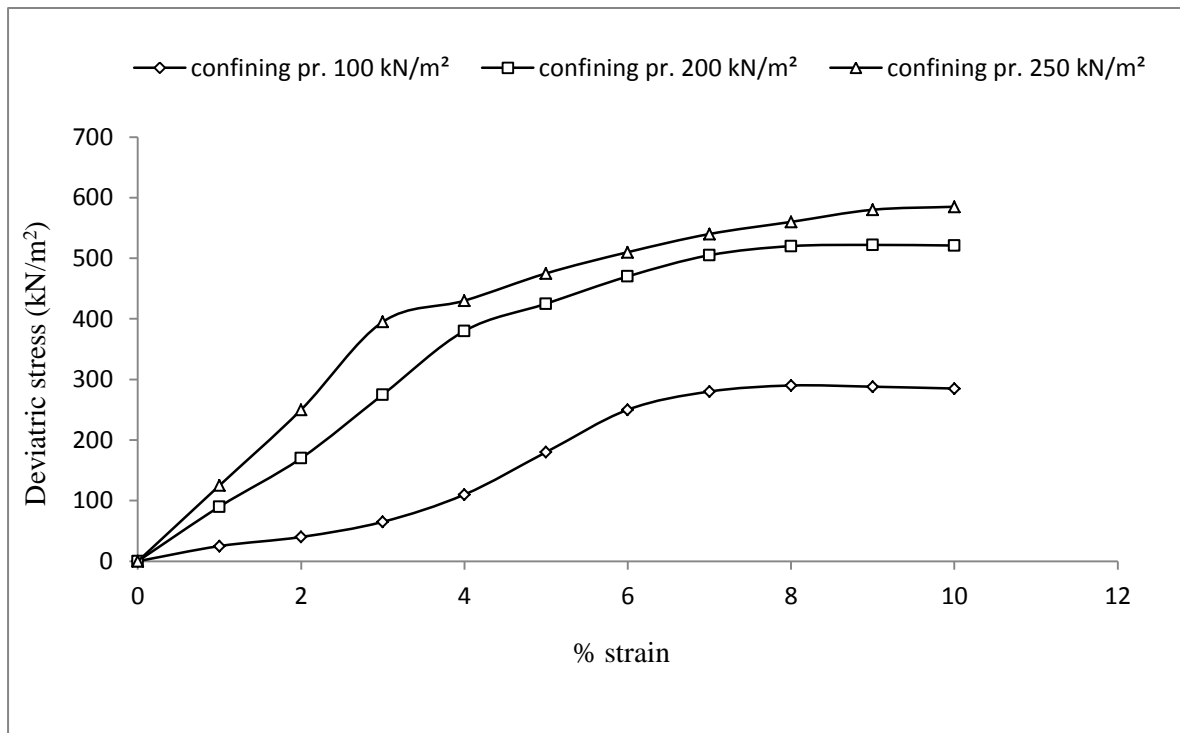


Fig.25 Stress-stain curve of DTU soil with woven geotextile.

5.7.3 UU test has been performed for soil with Non-woven geotextile reinforcement. It gives  $C=21.5\text{kN/m}^2$  and  $\Phi=17.6^\circ$ .



**Fig.26** Stress-strain curve of DTU soil with Non-woven geotextile



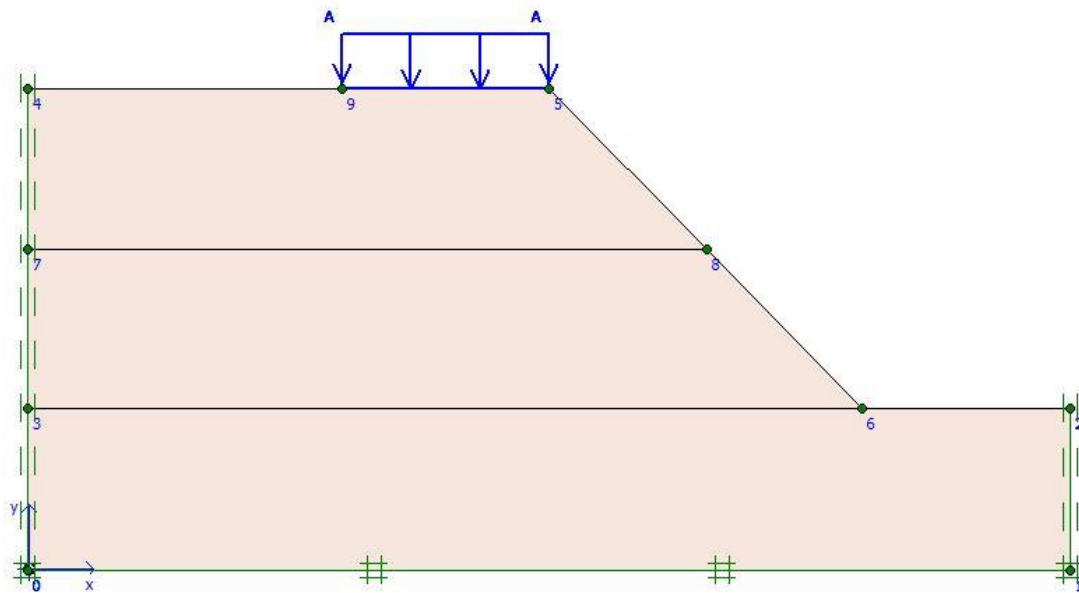
**Fig.27** soil sample in Triaxial test

**Table.9** physical properties of soil

Specific Gravity	2.60
Maximum Dry Density(kN/m <sup>3</sup> )	18.2
Optimum moisture content(%)	14
Direct Shear test	C =10.1 kN/m <sup>2</sup> , $\Phi$ =22.4 <sup>0</sup>
Triaxial test	C=11.3kN/m <sup>2</sup> , $\Phi$ =18.5 <sup>0</sup>
Soil classification	Silty sand(SM).

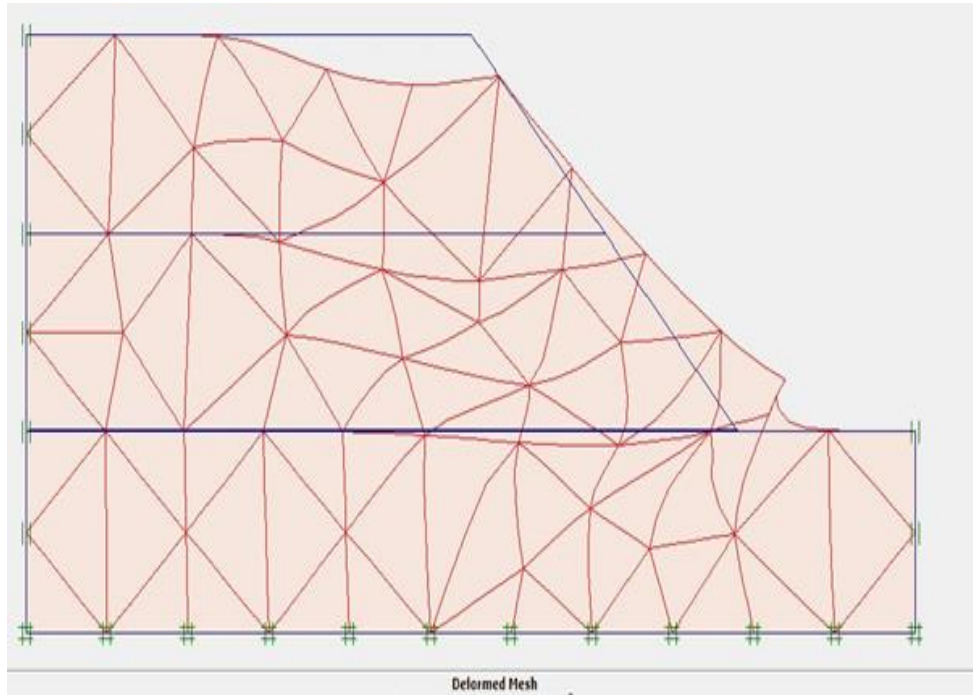
### 5.8 Numerical simulation

5.8.1 Numerical simulation is done with the help of PLAXIS software. In this problem slope angle is 45<sup>0</sup>.



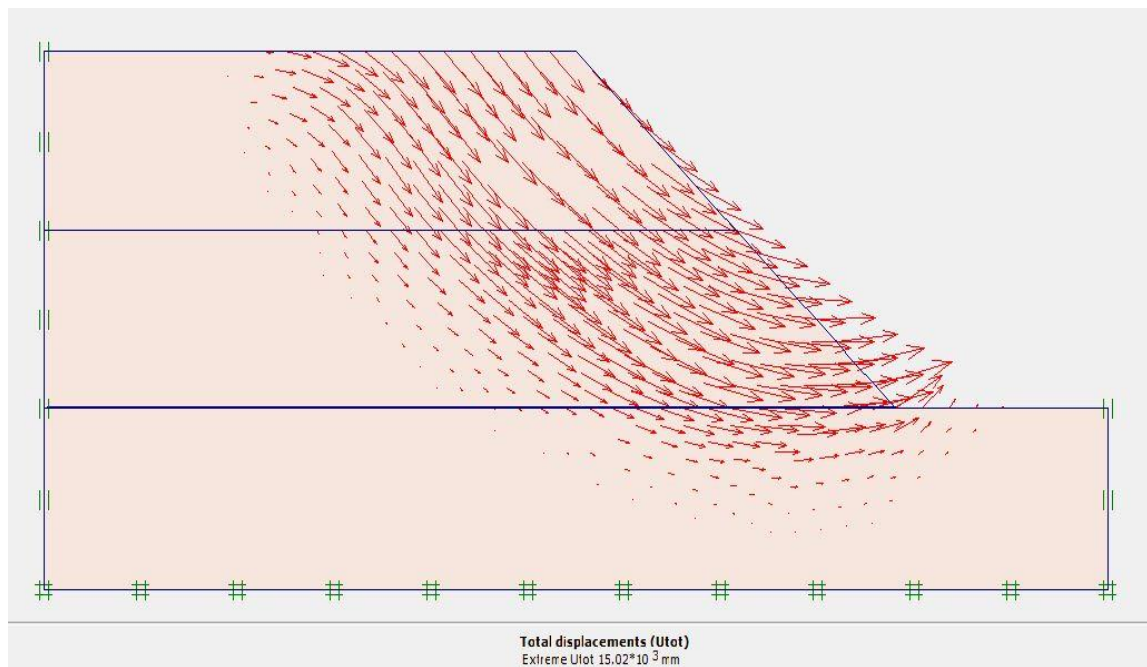
**Fig.28**Schematic view of test model at 45<sup>0</sup> slope angle

Above fig shows the model geometry which was tested in laboratory.



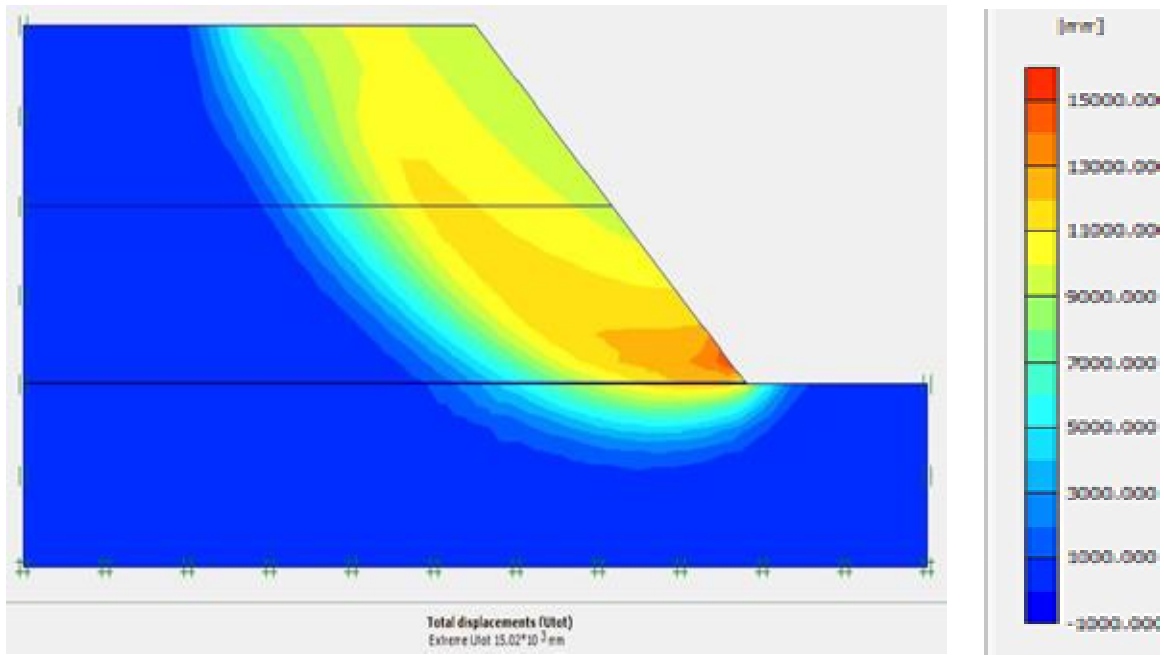
**Fig.29** Deformed mesh of model at  $45^{\circ}$  slope angle

Fig 29 shows the deformed model geometry after transferring the load. Soil particles gets settled vertically and move in horizontal direction.



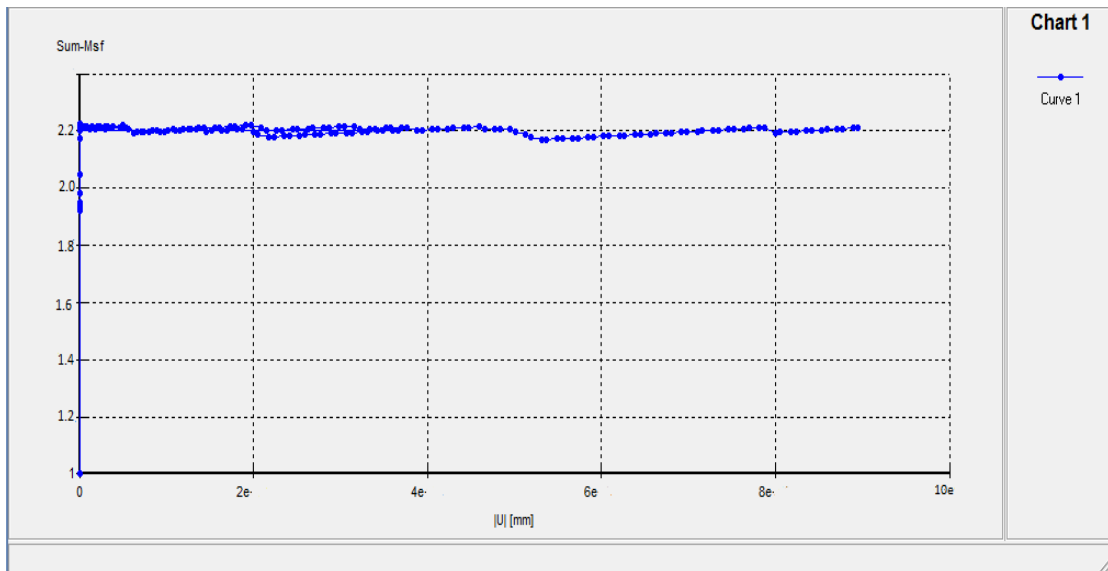
**Fig.30** Total displacement of model at  $45^{\circ}$  slope angle

Fig 30 shows horizontal displacement profile of soil particles. Soil particles moved in outward direction due load transfer causes the slope failure.



**Fig.31** Total shear strain shading with scale at  $45^0$  slope angle

Fig 31 shows total shear strain shading of soil particles and slope failure profile for the particular angle.

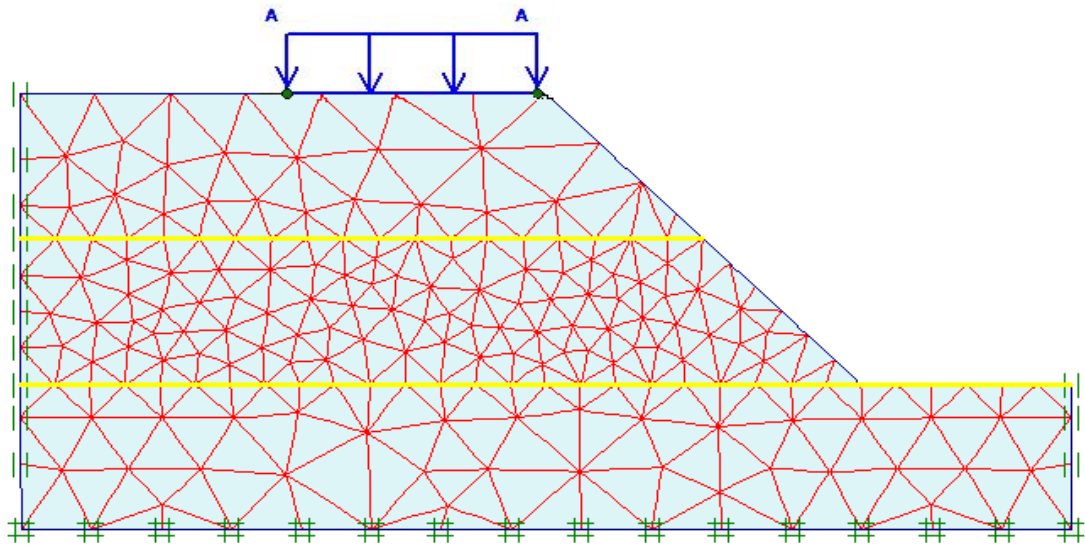


**Fig.32** factor of safety of unreinforced soil at  $45^0$  slope angle

Fig 32 represents the factor of safety against the deformation. The value of factor of safety is 2.2.

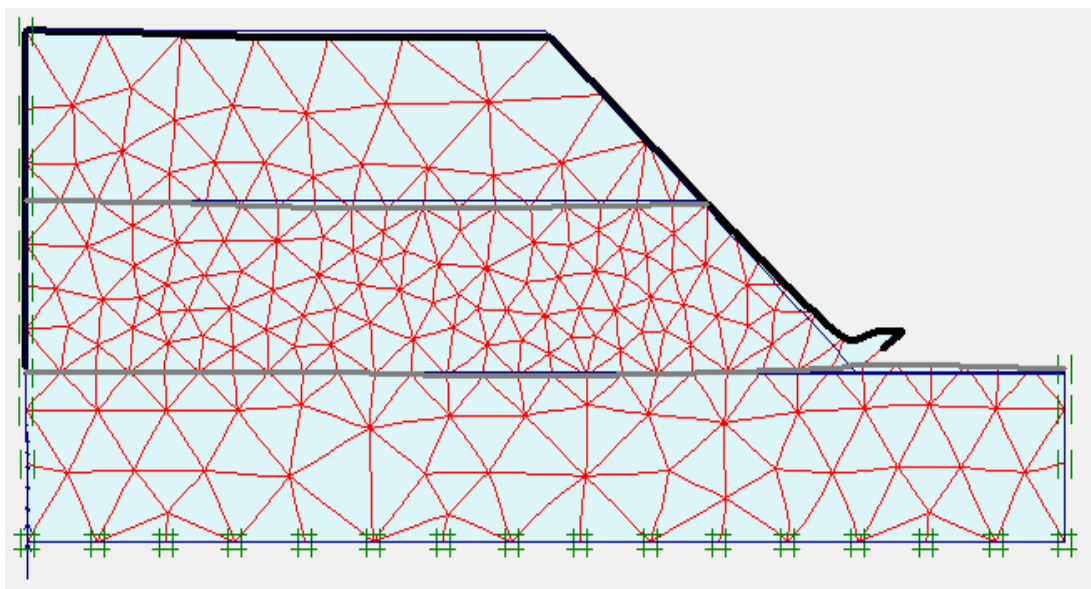
### 5.8.2 Model with Geotextile at 45° slope angle

A series of test is performed for the same model with reinforcement for slope angle 45°.



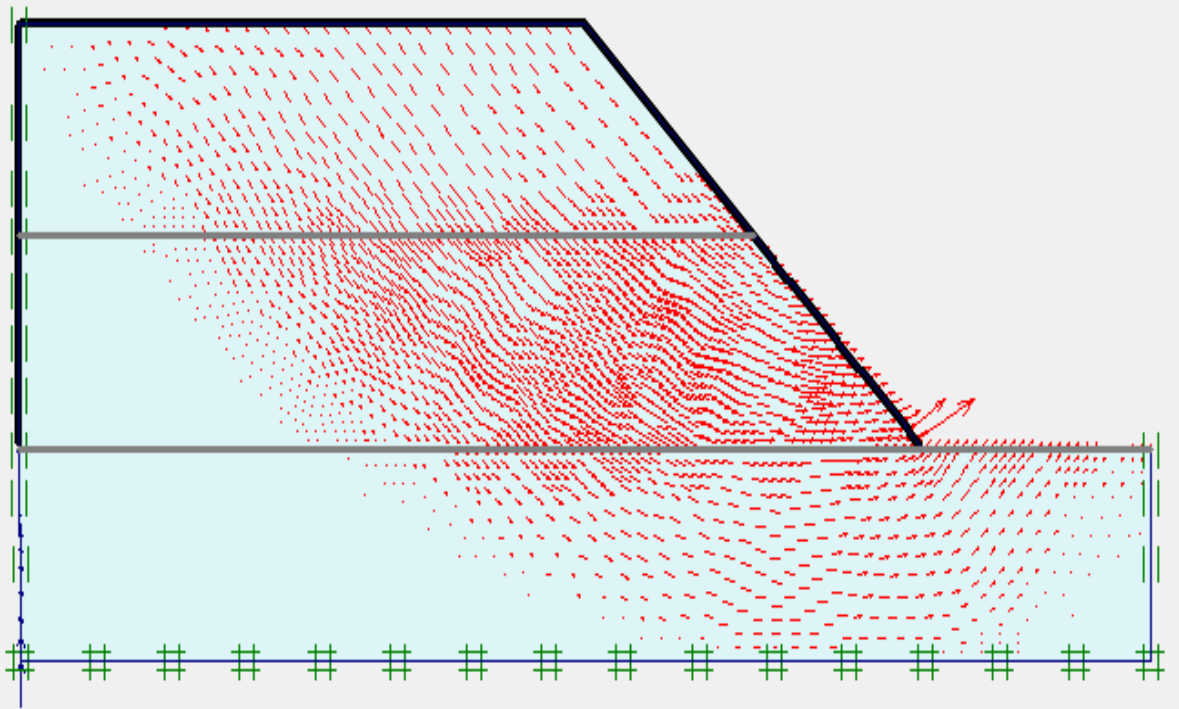
**Fig. 33** Schematic view of test model with geotextile at 45° slope angle

Fig 32 show model geometry with mesh and two layer of reinforcement. The reinforcement is provided by dividing total depth in three equal parts.



**Fig.34** Deformed mesh of model with geotextile at 45° slope angle





**Fig.35** Total displacement of model at 45° slope angle

Above two figs 34 and 35 shows model deformation and total displacement of soil particle with reinforcement.

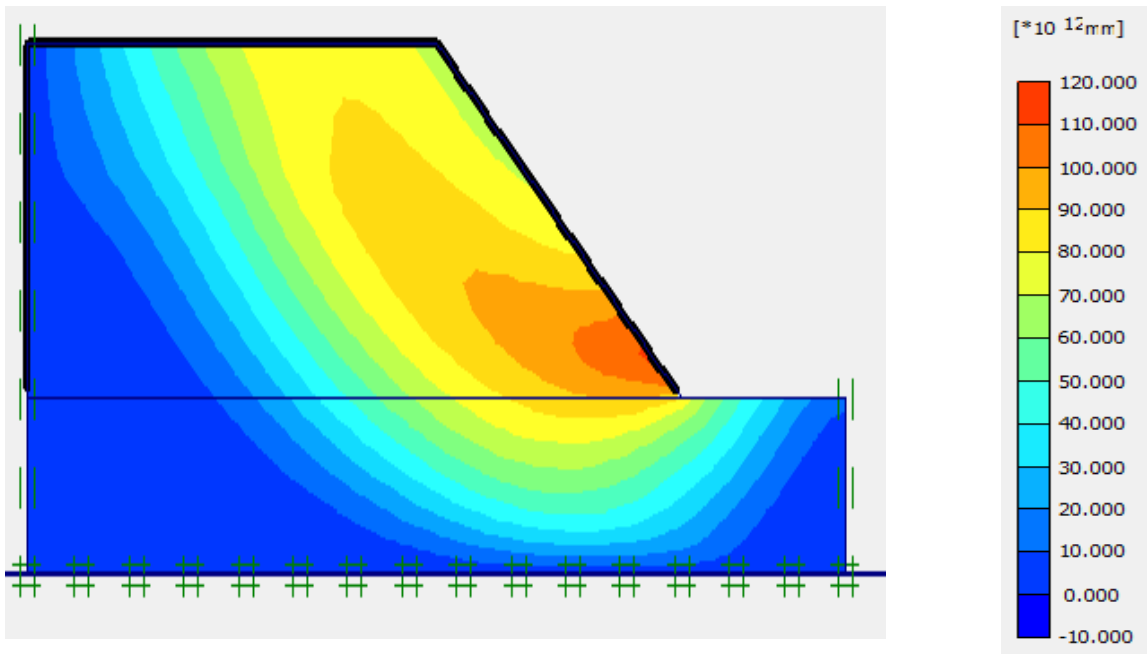


**Fig.36** Total shear strain shading with scale at 45° slope angle

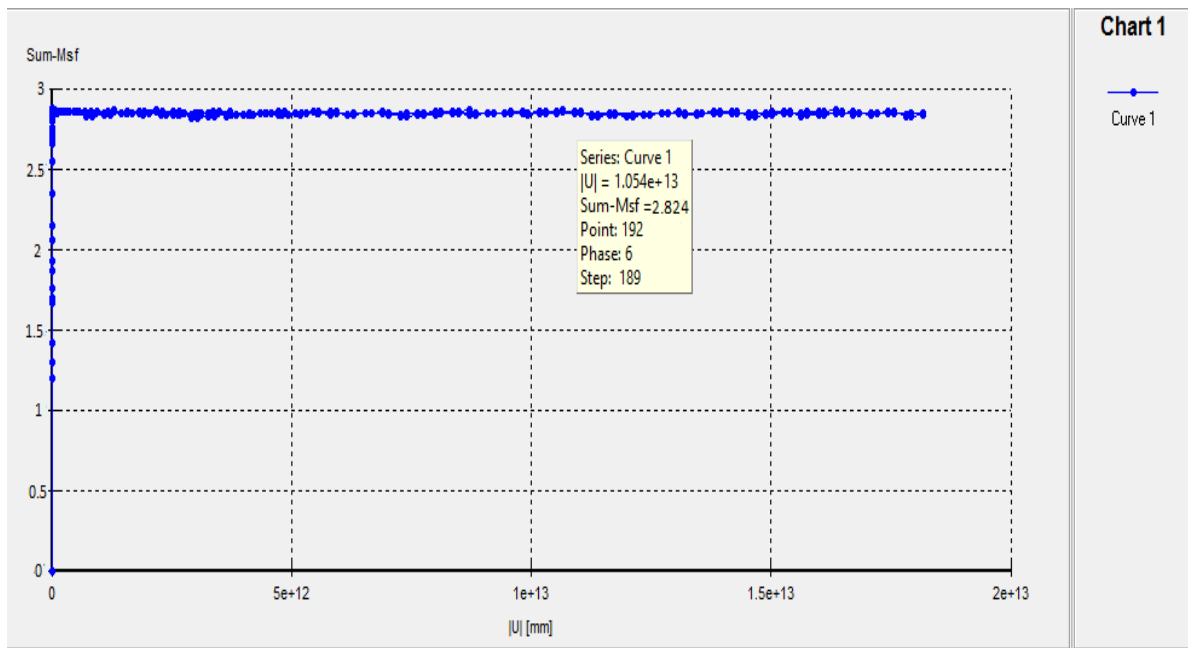


**Fig.37** factor of safety for testing model with geotextile at  $45^{\circ}$  slope angle

Figs 36 and 37 show slope failure profile and factor of safety with reinforcement for slope angle  $45^{\circ}$ . The factor of safety increased up to 2.8.

### 5.9 Model with slope angle $60^{\circ}$

5.9.1 In this problem slope angle is  $60^{\circ}$  and model is unreinforced.

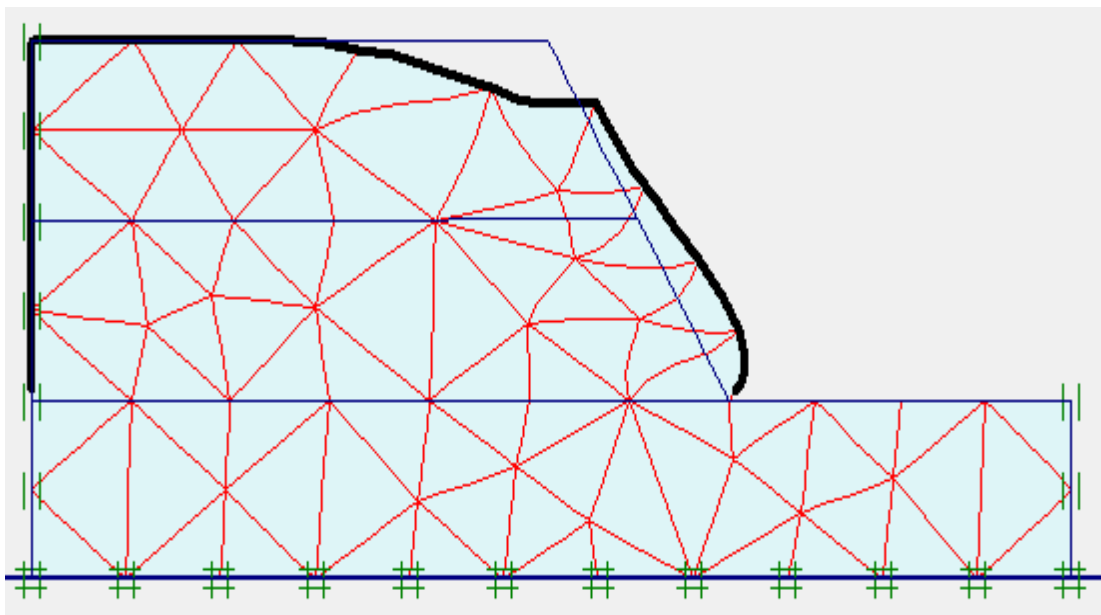


**Fig.38** Deformed mesh of model at  $60^{\circ}$  slope angle

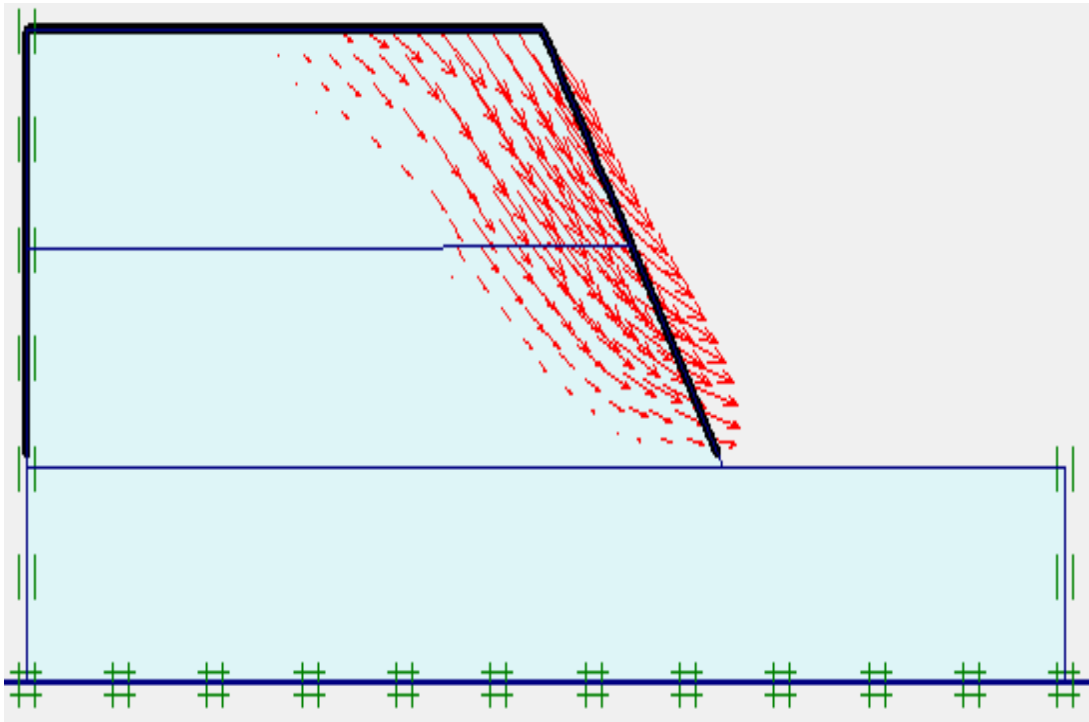


**Fig.39**Total displacement of model at 60<sup>0</sup> slope angle

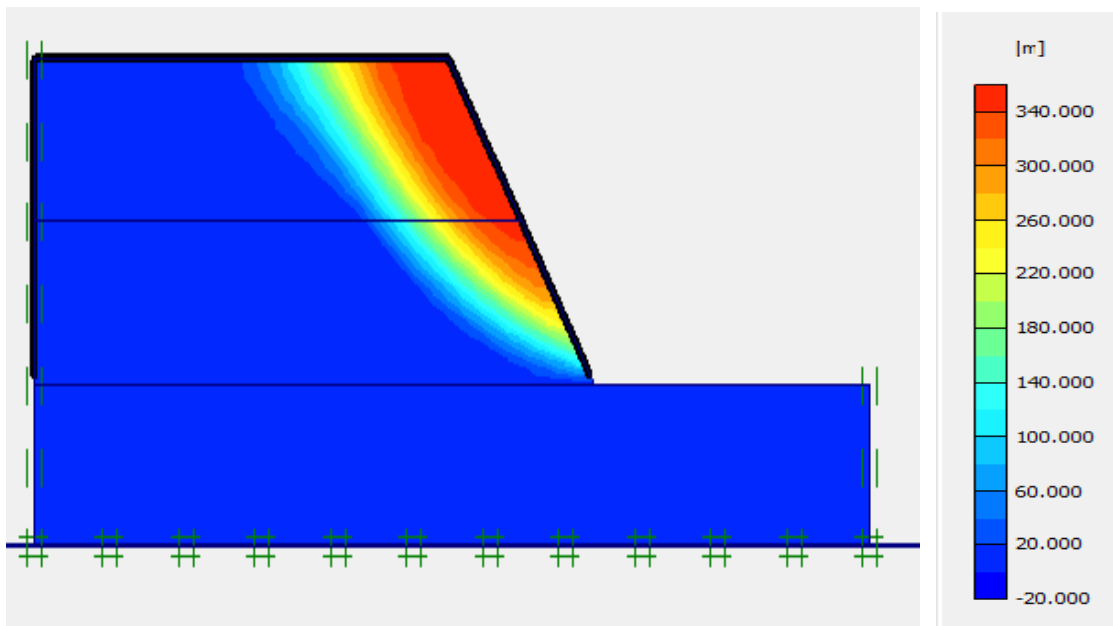


**Fig.40**Total shear strain shading with scale at 60<sup>0</sup> slope angle

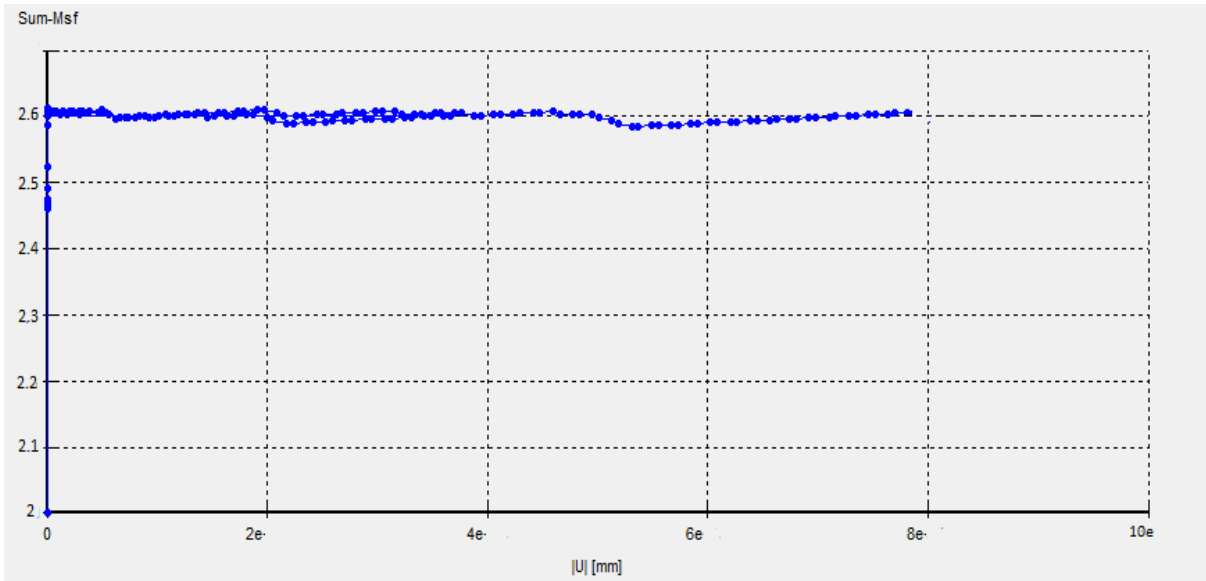


**Fig.41** factor of safety for testing model at 60° slope angle

### 5.9.2 Model with geotextile at 60° slope angle

This test is done with 60° slope angle and with reinforcement. Following fig shows the deformed layers of geotextile and soil slope.

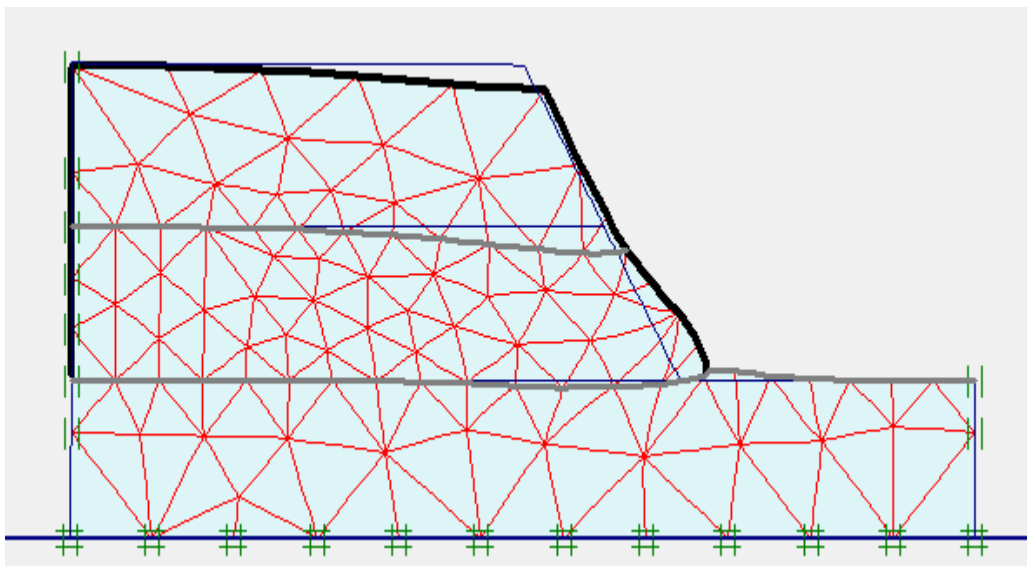


**Fig.42** Deformed mesh with reinforcement at 60° slope angle

Fig.42 shows deformation of soil slope in which soil particles moves in outward direction.

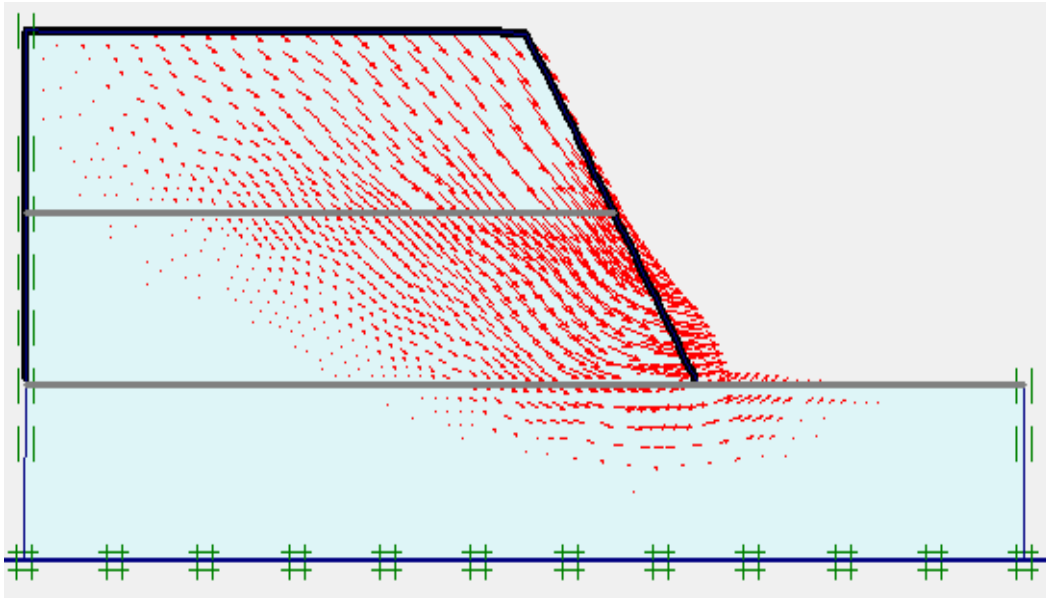


**Fig.43** Total deformation of slope with reinforcement at  $60^{\circ}$  slope angle

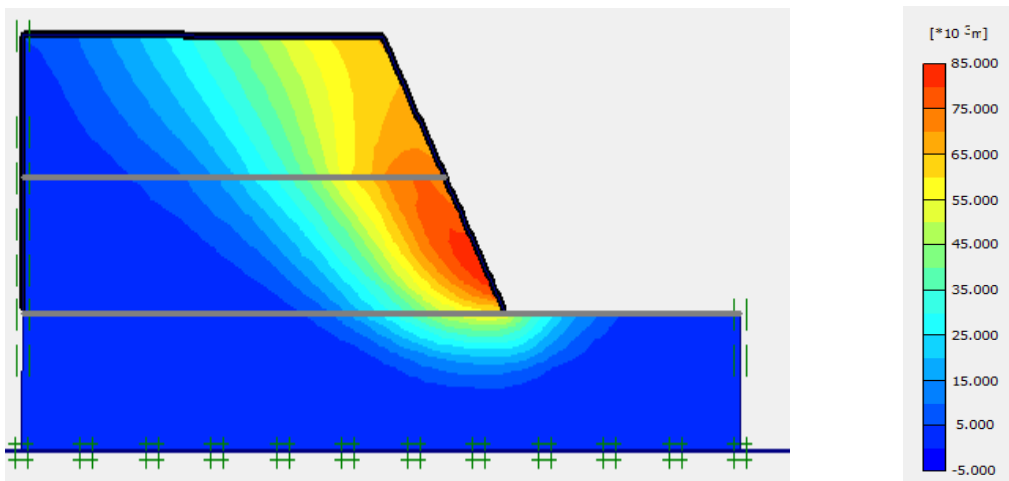


**Fig.44** Total strain shading with reinforcement at  $60^{\circ}$  slope angle

Fig44 gives the idea about failure surface of slope after the reinforcement.

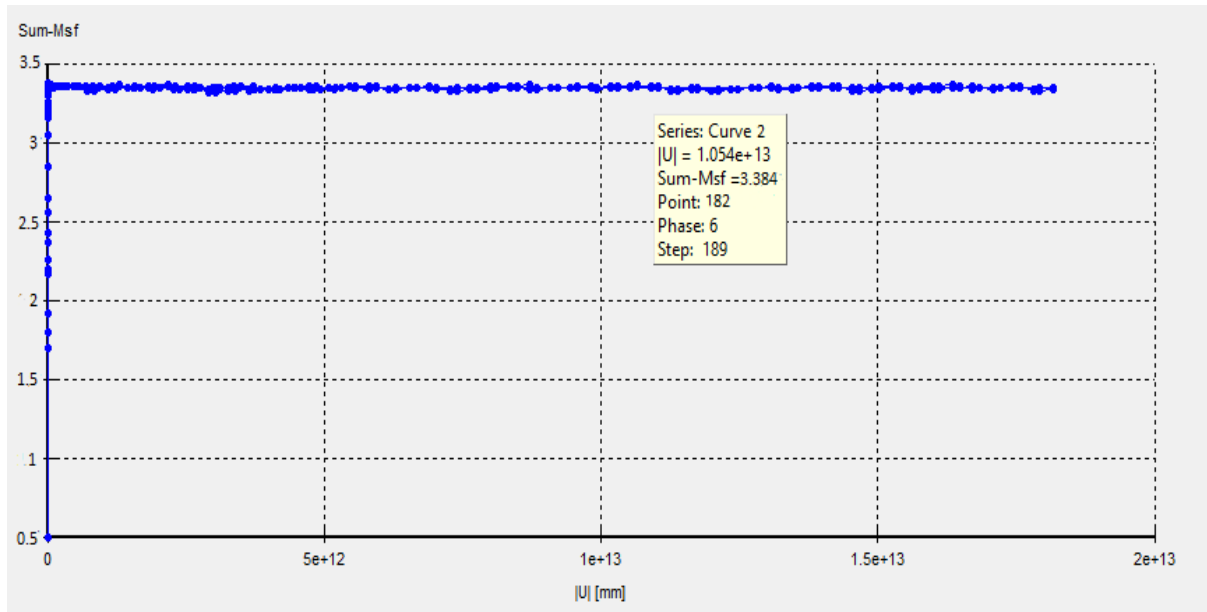


**Fig.45** factor of safety for testing model with reinforcement at 60° slope angle

## CHAPTER 6

### RESULTS AND DISCUSSION

**6.1 Test result for slope angle  $45^0$** - A series of test is performed in laboratory to find the effect of edge distances on slope failure for both reinforced and unreinforced slope. The corresponding edge distance are  $D/B=0, 1, 2$ .

By analysing the results it has been seen that as we provide the reinforcement layers, the load bearing capacity increases due to increase in its maximum dry density and Non-woven geotextiles shows better improvement results.

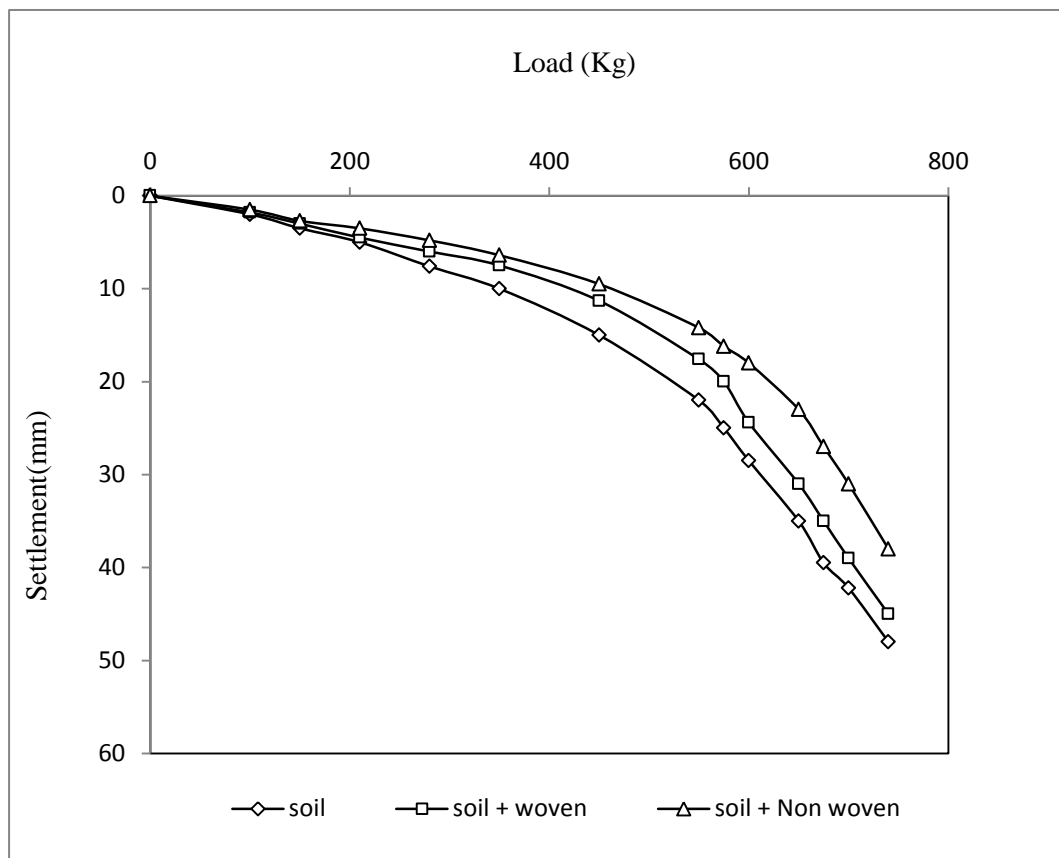


**Fig.46** Load- settlement curve for  $D/B=0$  with slope angle  $45^0$

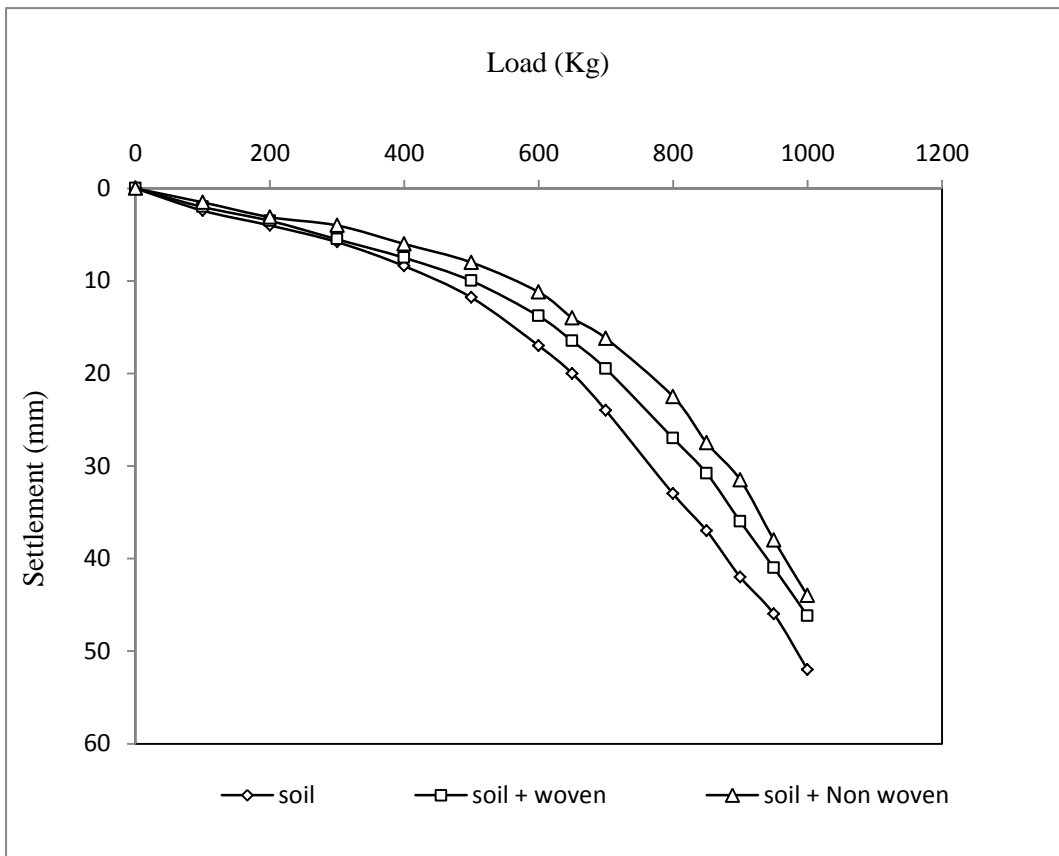


**Fig.47** Load-Settlement curve for D/B=1 with slope angle  $45^0$

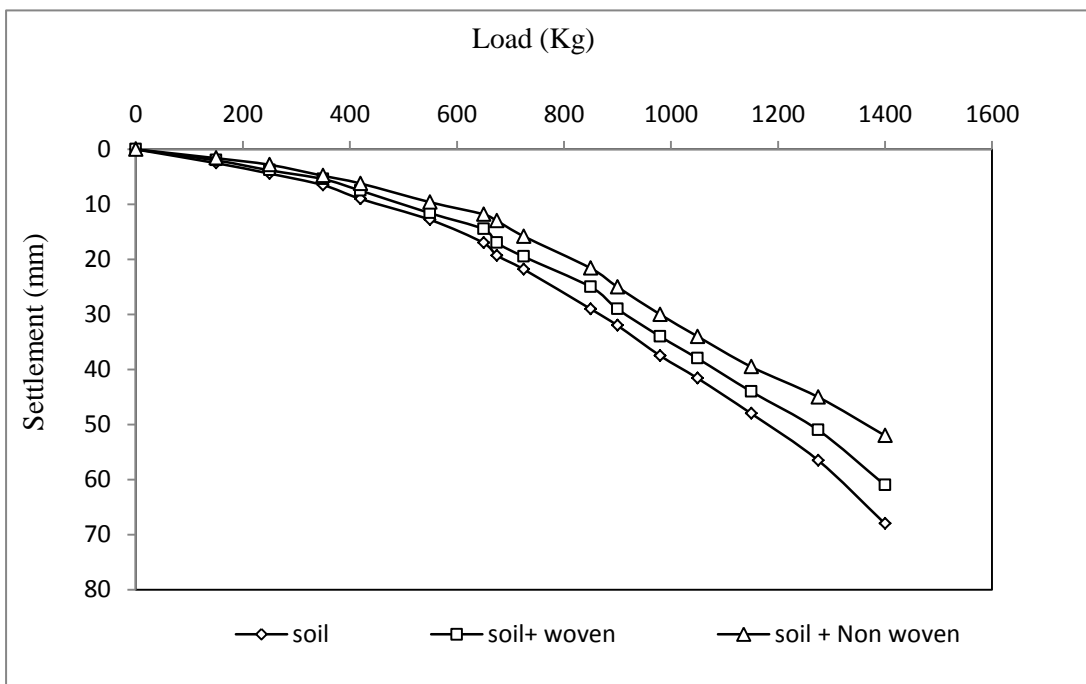


**Fig.48** Load-Settlement curve for D/B=2 with slope angle  $45^0$



As above results show that for  $D/B=0, 1, 2$ , the maximum load capacity is increases and settlement decreases with increase in edge distance.

**6.2 Test result for slope angle  $60^\circ$**  - Here for a different slope angle load-settlement curves are plotted for  $D/B=0, 1, 2$ .

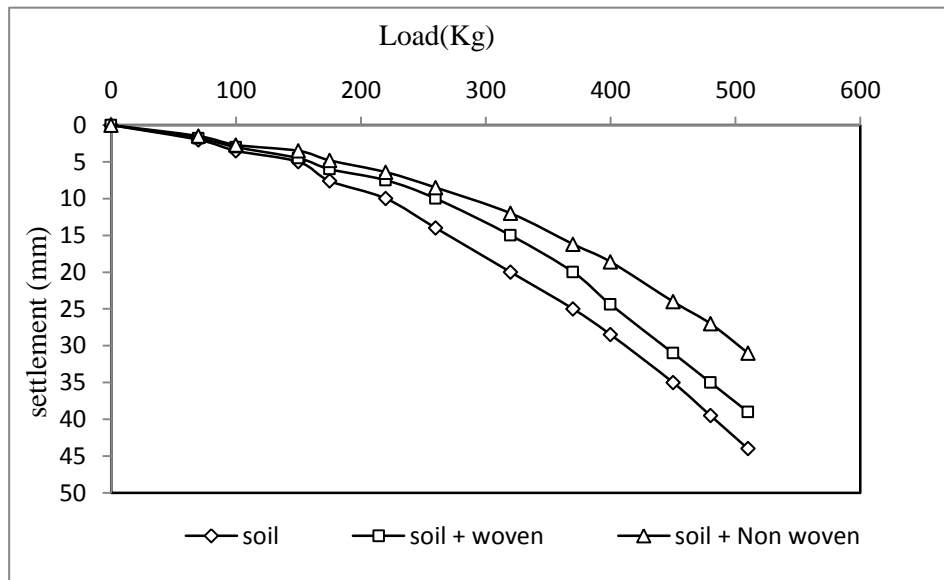


**Fig.49** Load- settlement curve for  $D/B=0$  with slope angle  $60^\circ$

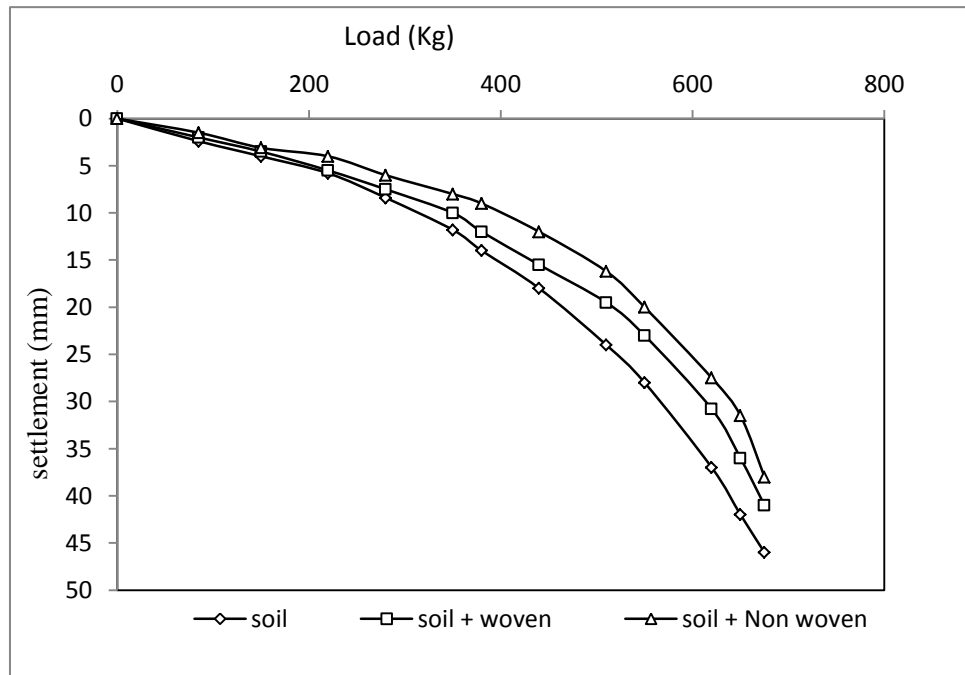


**Fig.50** Load- settlement curve for  $D/B=1$  with slope angle  $60^\circ$ .

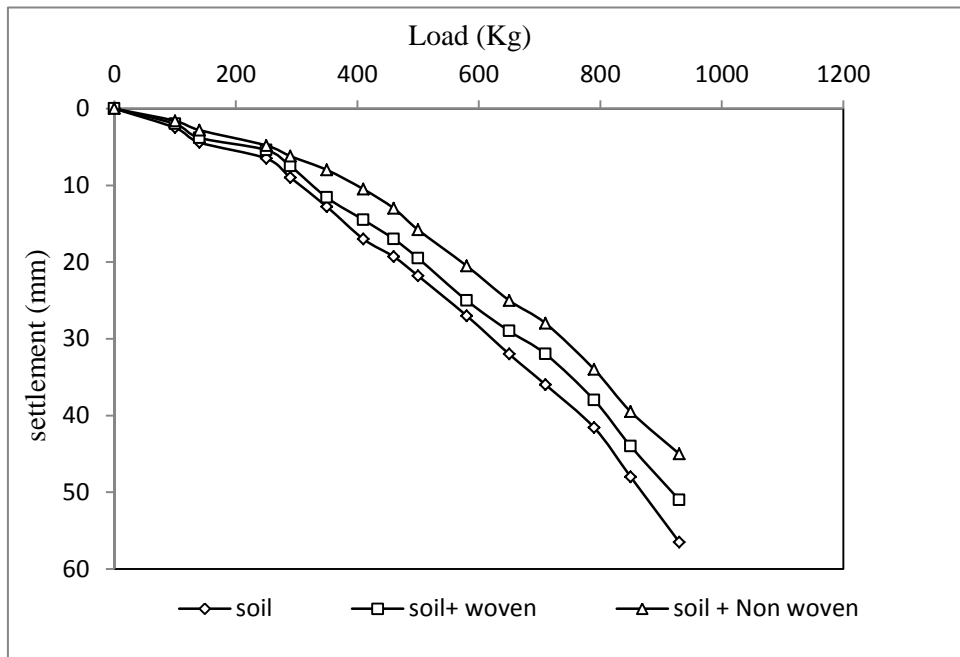


**Fig.51** Load- settlement curve for D/B=2 with slope angle  $60^{\circ}$ .

Here above plot shows that maximum loading capacity decreases with increase in slope angle.

For slope angle  $45^{\circ}$  and  $60^{\circ}$ , fig 53 shows that maximum loading capacity value with the variation of edge distance for two different slope angle . The effect of slope is minimised when the load is placed at an edge distance of two time of loading area. This change in load bearing capacity with change in edge distance can be explained by increasing passive earth pressure with increasing distance from slope. More passive pressures cause wider and deeper failure zones, thus increase in load bearing capacity.

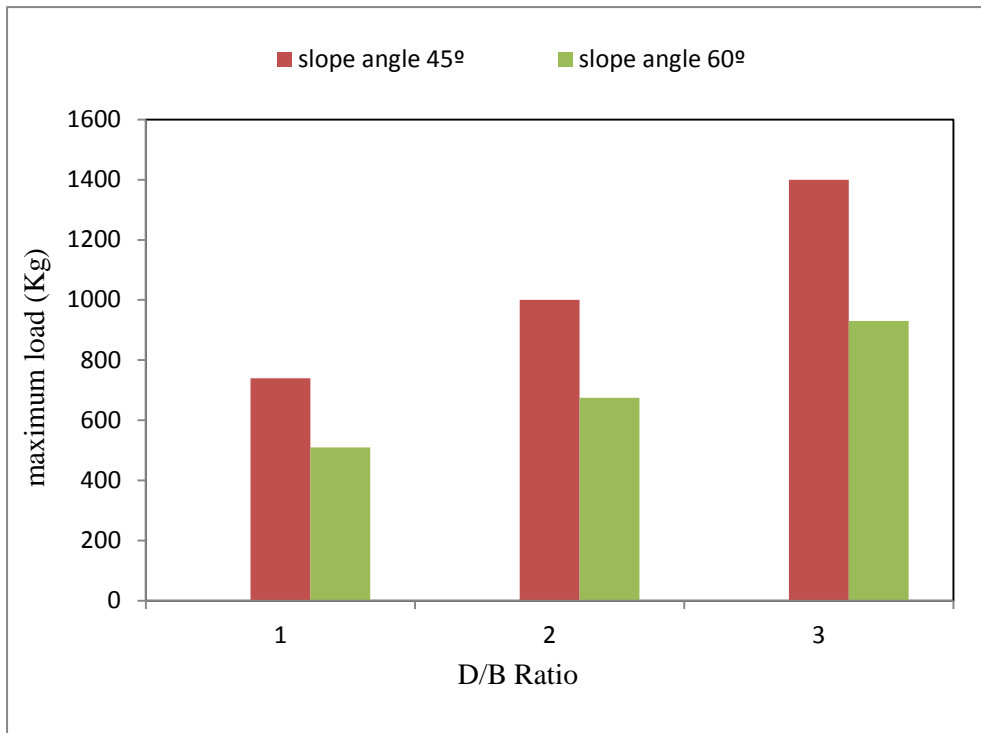


**Fig.52**Maximum load capacity for different edge distance

## CHAPTER 7

### CONCLUSION

A series of small scale laboratory model tests and numerical analysis have been done to investigate the load bearing capacity near slopes. The study focused on determining the effect of edge distance and sloping angle on stability of slope. On the basis of experimental and numerical studies, the following conclusions can be made-

- (1) The factor of safety for sloping angle  $45^{\circ}$  is 2.2 and 2.8 for unreinforced and reinforced slope respectively. Factor of safety increases up to 21.42 % for reinforced slope.
- (2) The factor of safety for sloping angle  $60^{\circ}$  is 2.6 and 3.3 for unreinforced and reinforced slope respectively. Factor of safety increases up to 21.1 %.
- (3) By analysing load-settlement curve for two different slope angle ( $45^{\circ}$  and  $60^{\circ}$ ), it is clearly indicate that the load carrying capacity is increases with increase in edge distance. For  $45^{\circ}$  angle it increases up to 53.5% and for  $60^{\circ}$  up to 42%.
- (4) Furthermore the curve shows that at a particular edge distance the ultimate load value is more for reinforced slope than unreinforced slope. Thus, use of reinforcement reflect the improvement in stability of slope.
- (5) Non-woven geotextile shows more ultimate load value than woven geotextile.
- (6) In DTU soil, reinforcement reduces the settlement value and increases the load carrying capacity. This can eliminate the instability problem.

## REFERENCES

- [1] Gorog and Torok, (2005) "Slope stability assessment of weathered clay by using field data and computer modelling" Nat. Hazards Earth Sys. Sci, 7, 417-422.
- [2] Fawaz A., Farah E., and Hagechehade F.(2014) "Slope stability analysis using numerical modelling" journal, ASCE, Vol.2, No.3, pp. 60-67.
- [3] Khan S.A., and Abbas M.S.(2014) "Numerical modelling of highway embankment", IJIRAE, Vol.1, issue 10, pp. 350-356.
- [4] Khanmahmadi S., and Hosseinitoudeshki "Effect of water table on stability of slope", journal, JNAS, Vol.3, No.11, pp.1237-1239.
- [5] Totsev A and Jevell J (2009) "Slope stability analysis using conventional methods and FEM" conference on soil mechanics.
- [6] Kainthola A, Verme D,(2013) " A review on numerical slope stability analysis", journal IJSETR, Vol.2, No.6., pp.1315-1320.
- [7] Khabbas H, Fatathi B, and Nucifora C (2007) "Finite element method against limit equilibrium approach for slope stability", UTS , Austria, pp.1293-1298.
- [8] Naeini S.A., Rabe B.K., and Mahmoodi E,(2012), "Bearing capacity and settlement of strip footing on geosynthetic reinforced clayey slopes", journal springer, j cent. South univ, Vol.19, pp.1116-1124.
- [9] Chauhya S.K., Singh R.S., Chakraborty M.K., and Dhar B.B.(1998), "Numerical modeling of biostabilisation for a coal mine overburden dump slope", ecological modeling, Vol.114, pp.275-286.

- [10] Tutluoglu L., and Karpuz C. (2008) “Investigation of large scale slope failure mechanism and numerical modeling for the safe design of slope in lignite mine”, International conference on Engineering Geology, Vol.8, pp.292- 300.
- [11] Rouaiguia A., and Dahim M.A., (2013), “Numerical modeling of slope stability analysis”, journal, IJESIT, Vol.2, Issue.3, pp.533-542.
- [12] Eftekari A., Taromi M., and Saeidi M. (2014), “Uncertainty and complexity of geological model in slope stability”, IJMGE, Vol. 48, No.1, pp 69-79.
- [13] Soren K., Budi G., and Sen P.(2014), “Stability analysis of a open pit”, IJRET, Vol.3, Issue 5, pp.326-334.
- [14] Chu H.K., Lo C.M., and Chang Y.L.(2013), “Numerical analysis of slope stability of a highway”, Journal of Chinese Soil and Water Conservation, Vol.42, No.2, pp.97-104.
- [15] Crosta G.B., Imposimato S., and Roddeman D.G. (2003), “Numerical modeling of large landslide stability and runout”, Natural hazards and earth system sciences Vol.3, pp.523-538.
- [16] IS: 2720 (Part 3) (1980). Methods of Test for Soils: Determination of Specific Gravity, Bureau of Indian Standards, New Delhi, India.
- [17] IS: 2720 (Part 7) (1980). Methods of Test for Soils: Determination of Water Content-Dry Density Relation Using Light Compaction, Bureau of Indian Standards, New Delhi, India.
- [18] IS: 2720 (Part 4) (1985). Methods of Test for Soils: Determination of Grain Size Analysis, Bureau of Indian Standards, New Delhi, India.
- [19] IS: 2720 (Part 13) (1986). Methods of Test for Soils: Determination of Friction angle and cohesion Using Direct shear test, Bureau of Indian Standards, New Delhi, India.